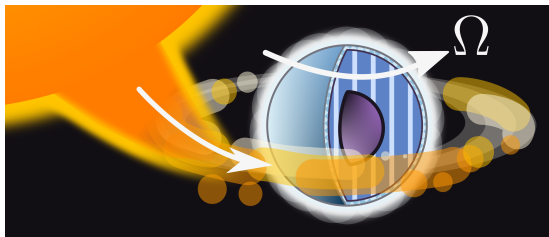


SUPERFLUID DYNAMICS IN NEUTRON STARS

ALLARD Valentin

PhD public defense (*May 21, 2024*)



Faculty
of
Sciences



Table of contents

1 Introduction

- Superfluidity in the laboratory
- Nuclear superfluidity in neutron stars

2 Nuclear energy-density functional theory

3 Gapless superfluidity

- Quasiparticle density of states and energy gap
- Impact on the specific heat

4 Astrophysical manifestation of gapless superfluidity

- Quasipersistent soft X-ray transients
- Specific heat and thermal timescale
- Results

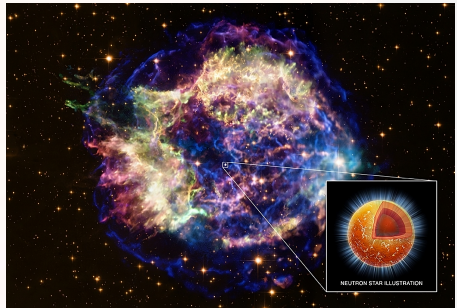
5 Conclusions and prospects

- Conclusions
- Prospects

Neutron stars

Formed in gravitational core-collapse supernova explosions. **Predicted in 1933** (Baade and Zwicky) and **observed in 1967** (Bell and Hewish)

- **Radius:** $R_{\text{NS}} \sim 10 \text{ km}$,
- **Mass:** $M_{\text{NS}} \sim 1.4 M_{\odot}$,
- **Density:** $\rho_{\text{NS}} \sim 10^{15} \text{ g/cm}^3$,
- **Energy scale (MeV):** $1 \text{ MeV} = 10^{10} \text{ K}$.
- **Temperature:** Initially very hot ($T \sim 100 \text{ MeV}$) but **cool down** to $T \sim 0.1 \text{ MeV}$, within days.

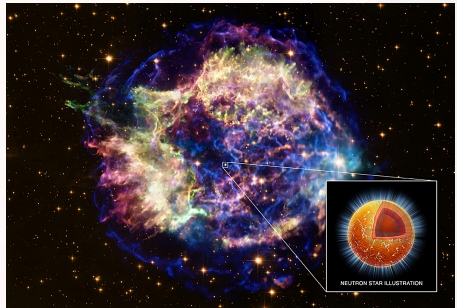


Cassiopeia A, credits: NASA/CXC/SAO

Neutron stars

Formed in gravitational core-collapse supernova explosions. **Predicted in 1933** (Baade and Zwicky) and **observed in 1967** (Bell and Hewish)

- **Radius:** $R_{\text{NS}} \sim 10 \text{ km}$,
- **Mass:** $M_{\text{NS}} \sim 1.4 M_{\odot}$,
- **Density:** $\rho_{\text{NS}} \sim 10^{15} \text{ g/cm}^3$,
- **Energy scale (MeV):** $1 \text{ MeV} = 10^{10} \text{ K}$.
- **Temperature:** Initially very hot ($T \sim 100 \text{ MeV}$) but **cool down** to $T \sim 0.1 \text{ MeV}$, within days.



Cassiopeia A, credits: NASA/CXC/SAO

Neutron stars contain **dense matter** which is expected to undergo various **phase transitions** such as **superfluidity**.

Superfluidity

First discovered in liquid ${}^4\text{He}$ (in the 1930's). Below the **critical temperature** $T_c = 2.17 \text{ K}$, helium does **not behave like an ordinary liquid.**"



Superfluid ${}^4\text{He}$ does not boil \implies **Non classical heat transport.**

Superfluidity

First discovered in liquid ^4He (in the 1930's). Below the **critical temperature** $T_c = 2.17 \text{ K}$, helium does **not behave like an ordinary liquid**. "



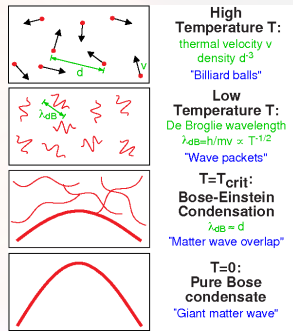
Flow without resistance through narrow slits and capillaries \Rightarrow **No viscosity**

Superfluidity and Bose Einstein Condensation (BEC)

In 1925, Bose and Einstein predicted that **below a critical temperature**, an ideal gas of **bosons** can **condense into a macroscopic quantum state**.

Link with ${}^4\text{He}$ superfluid

In 1938, London was the first to associate the BEC with ${}^4\text{He}$ superfluidity.



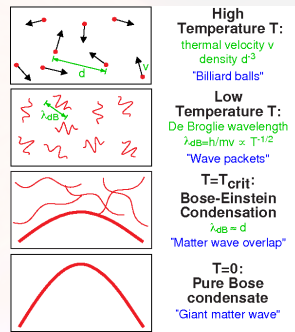
(Bose Einstein Condensate from MIT group)

Superfluidity and Bose Einstein Condensation (BEC)

In 1925, Bose and Einstein predicted that **below a critical temperature**, an ideal gas of **bosons** can **condense into a macroscopic quantum state**.

Link with ${}^4\text{He}$ superfluid

In 1938, London was the first to associate the BEC with ${}^4\text{He}$ superfluidity.



(Bose Einstein Condensate from MIT group)

Fermionic superfluidity ?

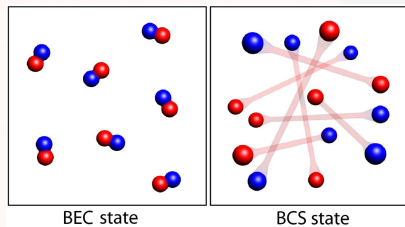
${}^3\text{He}$ superfluidity was observed at far lower temperatures ($T_c \sim \text{mK}$), in 1971
(Osheroff, Richardson and Lee, PRL 28, 885 (1972)) !

Bardeen Cooper Schrieffer theory

The **microscopic theory** of Bardeen, Cooper and Schrieffer (originally for electronic systems) was published in 1957 (1972 Nobel Prize in Physics).

Pair formation

A small attractive interaction leads to formation of **bosonic pairs** which condense below T_c .



Ketterle and Zwierlein, Riv. Nuovo Cimento., Vol. 31, Issue 5-6, p.247-422 (2018)

Pairing and superfluidity

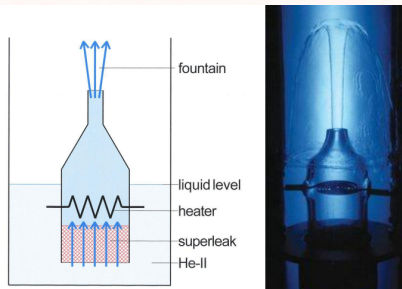
Fermionic superfluidity relies on the **pairing phenomena** and is described by the **binding energy of the pairs, Δ** .

Superfluid hydrodynamics

Tisza (1938) suggested that superfluid helium can be described by two inter-penetrating "fluids".

Tisza, Nature, 141: 913 (1938)

- A **superfluid**, carrying no entropy, with mass density $\rho^{(S)}$ and "Superfluid velocity" (momentum) V_S .
- A **normal viscous fluid**, carrying heat, with mass density $\rho^{(N)}$ and normal fluid velocity v_N .



Allen and Jones, Nature, 141:243 (1938)

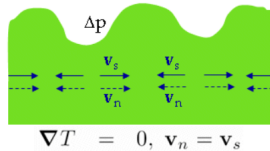
Superfluid hydrodynamics

Multifluid hydrodynamics

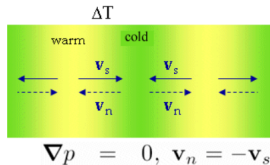
A superfluid contains **two** different **velocity fields**: \mathbf{v}_s and $\mathbf{v}_n \implies$ Two distinct modes/motions.

Tisza, *Nature* 141, 913; Landau, *Phys. Rev.* 60, 356.

first sound: pressure wave in bulk



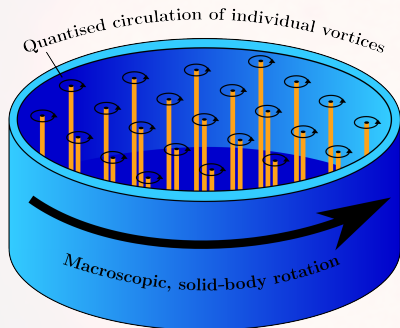
second sound: temperature wave in bulk



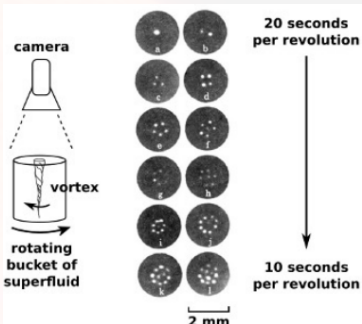
This explains the phenomenon of “temperature waves”.

Superfluid hydrodynamics

A rotating superfluid is threaded by an **array of quantum vortices**.



Graber and Andersson, International Journal of Modern Physics D, Vol. 26, No. 08, 1730015 (2017)



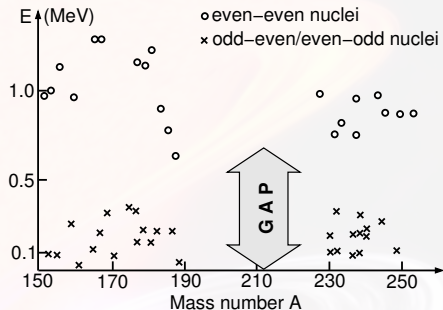
Yarmchuk et al., PRL 43:214–217 (1979)

Spinning-up (spinning-down) the superfluid is achieved by creating (destroying) vortices.

Nuclear superfluidity

Nuclear superfluidity was predicted well before the first discovery of neutron stars in 1967.

In 1957, Bohr, Mottelson, and Pines invoked the **nuclear pairing** to explain the **energy gap** in the excitation spectra of nuclei (first implication of superfluidity in the nuclear context).

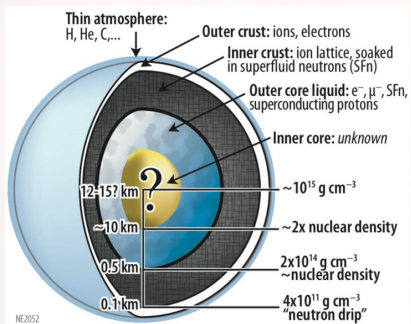


Bohr et al., Phys. Rev. 110, 936 (1958)

Neutron star superfluidity was also predicted by Migdal (1959) and studied by Ginzburg and Kirzhnits (1964) !

Nuclear superfluidity in neutron stars

Nuclear superfluidity predicted well before the discovery of neutron stars.

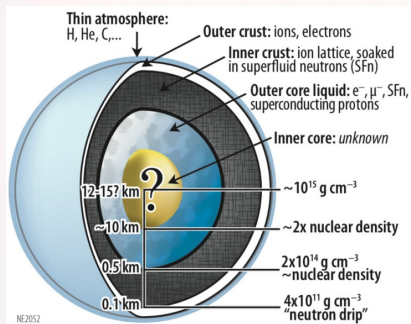


NASA, NICER Team

- Neutron superfluidity in the inner crust and **neutron-proton superfluid mixture** in the core.
- Impact on transport and thermal properties.
- **Superfluid neutrons weakly coupled** to the rest of the star
⇒ **Superfluid currents**.

Nuclear superfluidity in neutron stars

Nuclear superfluidity predicted well before the discovery of neutron stars.



NASA, NICER Team

- Neutron superfluidity in the inner crust and neutron-proton superfluid mixture in the core.
- Impact on transport and thermal properties.
- Superfluid neutrons weakly coupled to the rest of the star
⇒ **Superfluid currents.**

Most microscopic studies consider the neutron superfluid co-moving with the rest of the star.

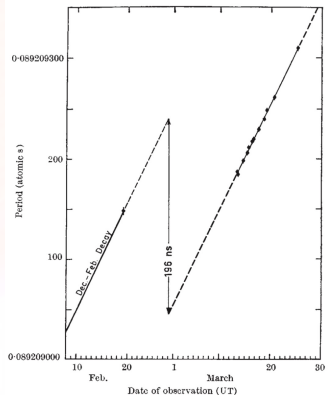
Pulsar frequency glitches

Pulsars are rotating neutron stars spinning with stable periods ($\dot{P} \gtrsim 10^{-12}$)
BUT.

Pulsar glitches

Sudden **decrease** of spin period of pulsars (rotating NS) interpreted as the **manifestation of superfluid dynamics**.

Antonopoulou et al., Rep. Prog. Phys., 85(12), 126901 (2022)



Radhakrishnan and Manchester, Nature, 222:228–229

(1969)

Pulsar frequency glitches

Pulsars are rotating neutron stars spinning with stable periods ($\dot{P} \gtrsim 10^{-12}$)
BUT.

Pulsar glitches

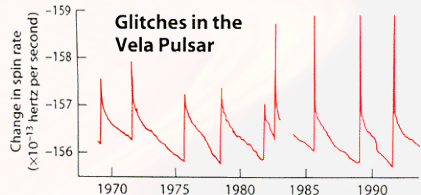
Sudden **decrease** of spin period of pulsars (rotating NS) interpreted as the **manifestation of superfluid dynamics**.

Antonopoulou et al., Rep. Prog. Phys., 85(12), 126901 (2022)

So far, 674 glitches (in 225 pulsars) have been detected.

[http:](http://www.jb.man.ac.uk/pulsar/glitches.html)

[//www.jb.man.ac.uk/pulsar/glitches.html](http://www.jb.man.ac.uk/pulsar/glitches.html)



A. Lyne & F. Graham-Smith, Pulsar astronomy 48, Cambridge University Press (2012)

Pulsar frequency glitches

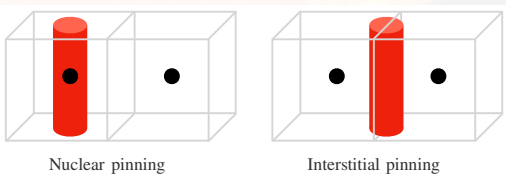
Explained by a transfer of angular momentum between a superfluid component and a “normal” component.

Anderson and Itoh, Nature, 256:25–27 (1975)

- Superfluid component (rotating with Ω_n) threaded by quantized vortices.

Superfluid vortices can pin to nuclei (or between them) in the crust.

Klausner et al., PRC 108, 035808 (2023)



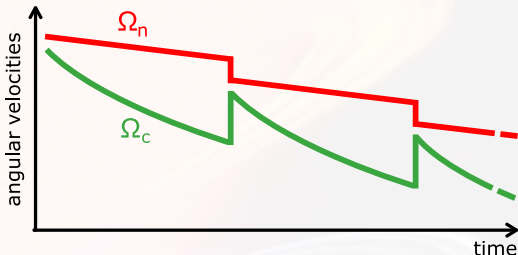
JCAP, Vol. 2024, Issue 03, id.051, 32 pp (2024)

Pulsar frequency glitches

Explained by a transfer of angular momentum between a superfluid component and a “normal” component.

Anderson and Itoh, Nature, 256:25–27 (1975)

- Superfluid component (rotating with Ω_n) threaded by quantized vortices.
- Normal component made of the (non-superfluid) crust and charged particles tightly coupled (rotating with Ω_c).



Sourie et al., PRD 93:083004 (2016)

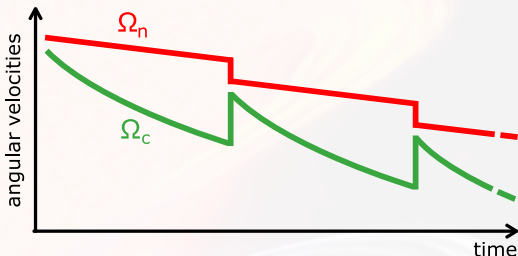
Glitches triggered by catastrophic vortex unpinning caused by an increasing lag $\Omega_n - \Omega_c$.

Pulsar frequency glitches

Explained by a transfer of angular momentum between a superfluid component and a “normal” component.

Anderson and Itoh, Nature, 256:25–27 (1975)

- Superfluid component (rotating with Ω_n) threaded by quantized vortices.
- Normal component made of the (non-superfluid) crust and charged particles tightly coupled (rotating with Ω_c).



Sourie et al., PRD 93:083004 (2016)

The very long post-glitch relaxation (from days to years) also provided the evidence for superfluidity.

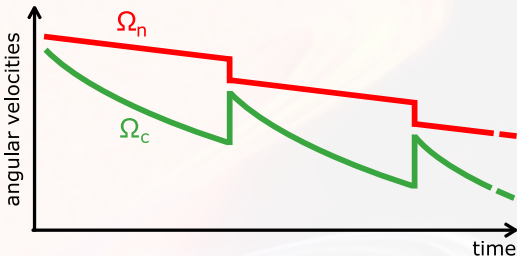
Baym et al., Nature 224, 673 (1969)

Pulsar frequency glitches

Explained by a transfer of angular momentum between a superfluid component and a “normal” component.

Anderson and Itoh, Nature, 256:25–27 (1975)

- Superfluid component (rotating with Ω_n) threaded by quantized vortices.
- Normal component made of the (non-superfluid) crust and charged particles tightly coupled (rotating with Ω_c).



Sourie et al., PRD 93:083004 (2016)

Currents induced by the lag $\Omega_n - \Omega_c$ could exceed a critical value and destroy superfluidity.

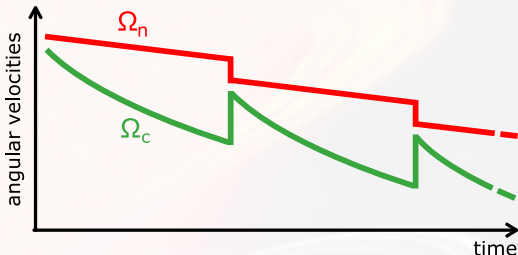
Sedrakian and Cordes, MNRAS, 307:365–375 (1999)

Pulsar frequency glitches

Explained by a transfer of angular momentum between a superfluid component and a “normal” component.

Anderson and Itoh, Nature, 256:25–27 (1975)

- Superfluid component (rotating with Ω_n) threaded by quantized vortices.
- Normal component made of the (non-superfluid) crust and charged particles tightly coupled (rotating with Ω_c).



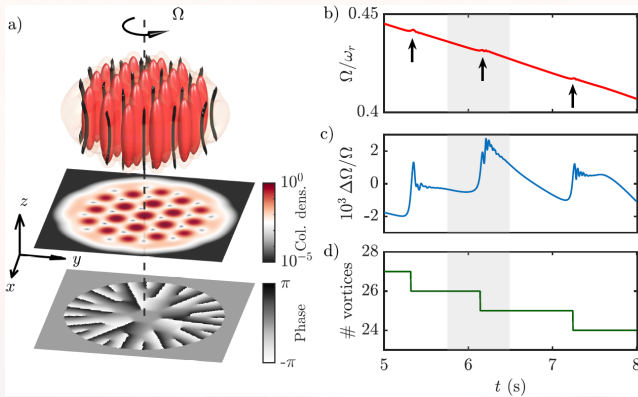
Sourie et al., PRD 93:083004 (2016)

Glitch-like behaviors have also been observed in superfluid helium.

Tsakadze and Tsakadze, J. Low Temp. Phys. 39 (1980)

Pulsar frequency glitches

Glitches were also recently simulated using ultracold atoms.

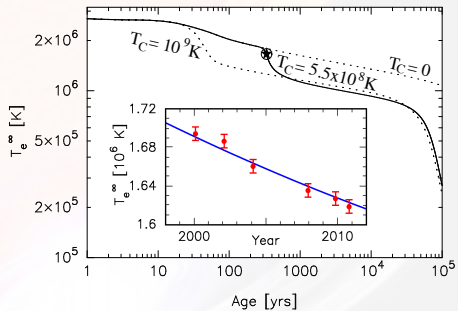
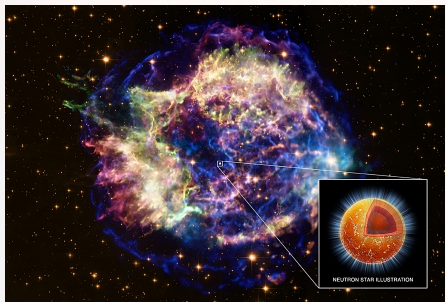


Poli et al., PRL 131, 223401 (2023)

Cooling of Cassiopeia A

The fast cooling of the Cassiopeia A remnant suggests a recent transition to
Nuclear superfluidity.

Page et al., PRL 106, 081101; Shternin et al., MNRAS 412, L108; Ho et al., MNRAS 506, 5015; Posselt et al., ApJ. 932, 83



How do finite superflows influence the critical temperature T_c ?

Aims

- Consistent determination of microscopic inputs for hydrodynamic simulations of superfluid neutron stars.

Aims

- Consistent determination of microscopic inputs for hydrodynamic simulations of superfluid neutron stars.
- Study of the disappearance of superfluidity.

Aims

- Consistent determination of microscopic inputs for hydrodynamic simulations of superfluid neutron stars.
- Study of the disappearance of superfluidity.
- Application to the cooling of transiently accreting neutron stars.

Mass current and entrainment effects

Superfluid neutrons (n) and protons (p) in a neutron star are mutually coupled by non-dissipative entrainment effects.

Gusakov and Haensel, Nucl. Phys. A, 761:333–348 (2005)

Similar effects were also found in superfluid ^3He - ^4He mixture.

Andreev and Bashkin, Sov. Phys. JETP 42, 164 (1975)

Mass current and velocity fields (superfluid mixtures)

Mass currents ρ_q (with $q = n, p$) are not simply aligned to their associated superfluid velocities V_q .

$$\rho_n = \rho_n^{(N)} \mathbf{v}_N + \rho_{nn} V_n + \rho_{np} V_p ,$$

$$\rho_p = \rho_p^{(N)} \mathbf{v}_N + \rho_{pp} V_p + \rho_{pn} V_n ,$$

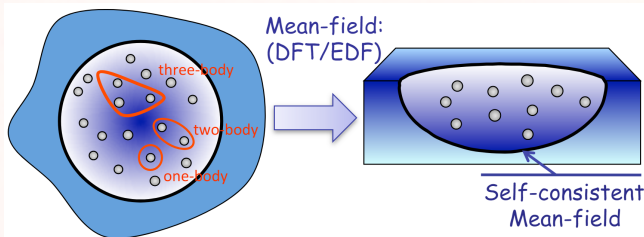
$\rho_{qq'}$ = Entrainment matrix

$\rho_q^{(N)}$ = Normal density

Energy-density functional theory

The Nuclear energy-density functional theory allows for a self-consistent treatment of nuclear superfluidity in the crust and in the core.

Potekhin *et al.*, A&A, 560:A48 (2013); Fantina *et al.*, A&A, 620:A105 (2018)



Philosophy of the energy-density functional theory

Strongly interacting particles (N -body problem) \Rightarrow **weakly interacting quasiparticles** characterized by the quasiparticle energy \mathcal{E} .

Energy-density functional theory

The total energy E of a neutron-proton (superfluid) mixture = functional of various densities and currents whose minimization leads to highly non-linear equations.

In principle exact BUT the **exact functional** remains **to be determined**.

Energy-density functional theory

The total energy E of a neutron-proton (superfluid) mixture = functional of various densities and currents whose minimization leads to highly non-linear equations.

In principle exact BUT the **exact functional** remains **to be determined**.

Homogeneous solutions

For hot **homogeneous neutron-proton superfluid mixture** with stationary flows, we obtained exact solutions !

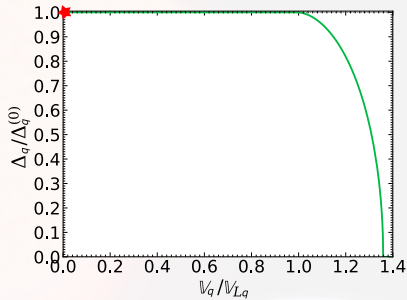
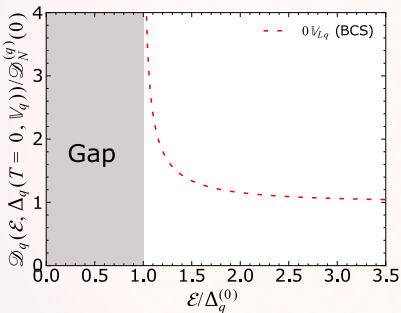
Allard and Chamel, PRC 103, 025804 (2021)

- The quasiparticles depend on T and on the **effective superfluid velocity** \mathbf{V}_q (manifestation of currents and entrainment effects).
- Universal results have been obtained for Δ_q and for the entrainment matrix $\rho_{qq'}$, for finite temperature and currents !

Allard and Chamel, Universe 7(12) (2021)

Gapless superfluidity

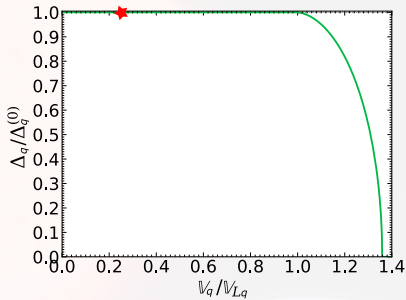
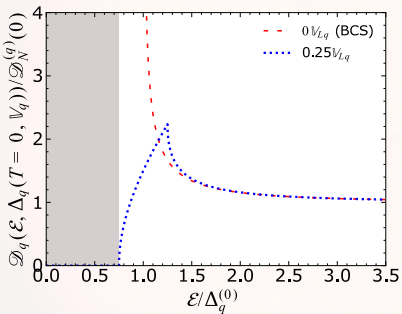
Finite currents influence the quasiparticle density of states $\mathcal{D}_q(\mathcal{E}, \Delta_q)$.



Energy **gap** = Forbidden region in the quasiparticle density of states.

Gapless superfluidity

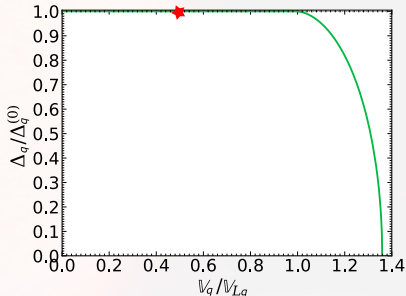
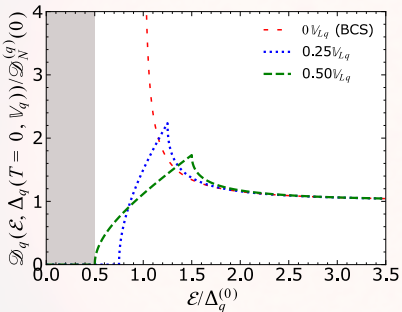
Finite currents influence the quasiparticle density of states $\mathcal{D}_q(\mathcal{E}, \Delta_q)$.



The energy gap shrinks with increasing \mathbb{V}_q

Gapless superfluidity

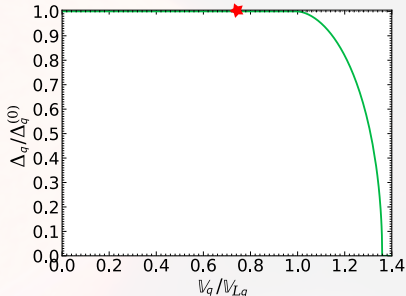
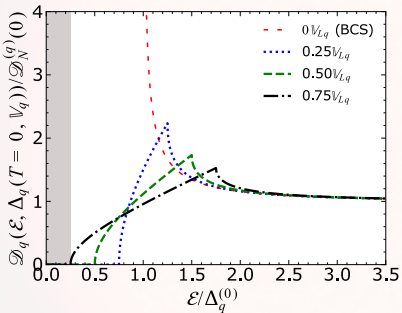
Finite currents influence the quasiparticle density of states $\mathcal{D}_q(\mathcal{E}, \Delta_q)$.



The energy gap shrinks with increasing \mathbb{V}_q

Gapless superfluidity

Finite currents influence the quasiparticle density of states $\mathcal{D}_q(\mathcal{E}, \Delta_q)$.



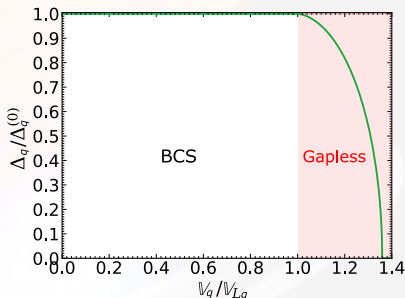
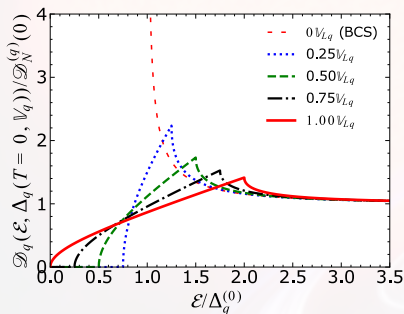
The energy gap shrinks with increasing \mathbb{V}_q

Gapless superfluidity

Gapless regime

The energy gap disappears at Landau's velocity V_{Lq} but superfluidity is only destroyed at $V_{cq}^{(0)} \simeq 1.36V_{Lq}$.

Allard and Chamel, PRC 108, 015801 (2023)

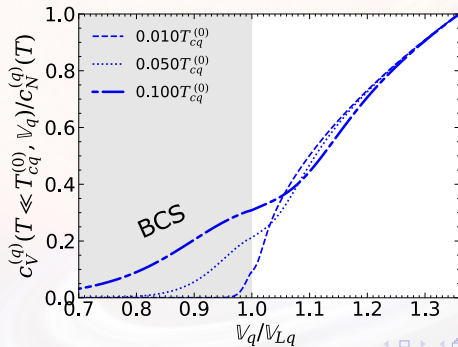


A normal fluid is present even at $T = 0$. Allard and Chamel, PRC 108, 045801 (2023)

Gapless superfluidity and specific heat

Low velocities ($V_q < V_{Lq}$)

The specific heat $c_V^{(q)}(T, V_q)$ is **exponentially suppressed** (compared to associated specific heat in non-superfluid phase $c_N^{(q)}(T)$).

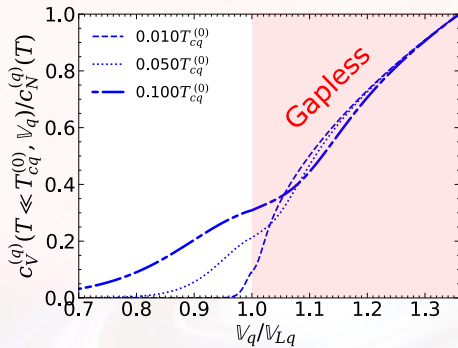


Gapless superfluidity and specific heat

Gapless regime ($\mathbb{V}_{Lq} \leq \mathbb{V}_q \lesssim 1.36 \mathbb{V}_{Lq}$)

- The specific heat $c_V^{(q)}$ becomes comparable to $c_N^{(q)}(T)$.

Allard and Chamel, PRC 108, 015801 (2023)

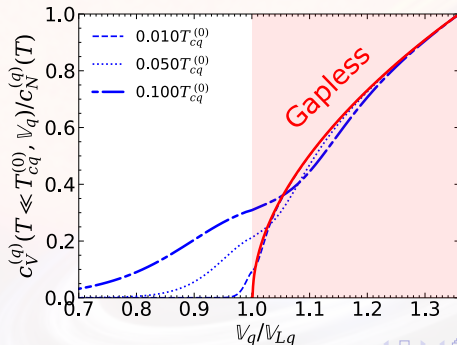


Gapless superfluidity and specific heat

Gapless regime ($\mathbb{V}_{Lq} \leq \mathbb{V}_q \lesssim 1.36\mathbb{V}_{Lq}$)

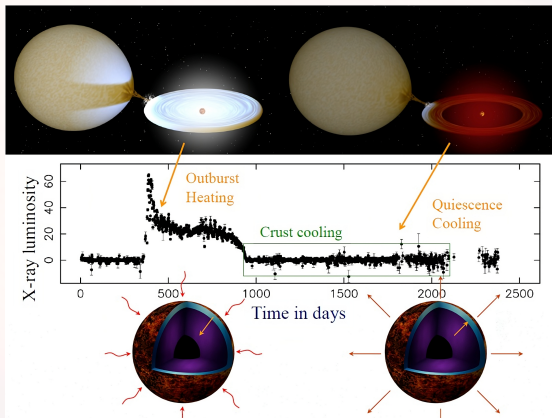
- The specific heat $c_V^{(q)}$ becomes comparable to $c_N^{(q)}(T)$.
- **Universal expression** for $c_V^{(q)}(T, \mathbb{V}_n)/c_N^{(q)}(T)$ as a function of $\mathbb{V}_q/\mathbb{V}_{Lq}$.

Allard and Chamel, PRC 108, 015801 (2023)



Application: Quasipersistent soft X-ray transients

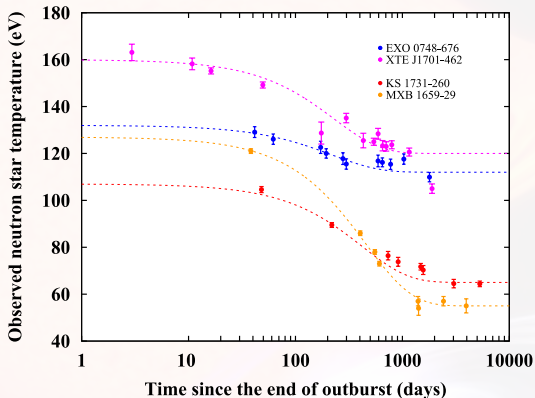
Neutron star crust heated during **accretion regime** (for $\sim 1\text{-}10$ years) before **cooling phase**.



Wijnands et al., J. Astrophys. Astr. 38: 49 (2017)

Application: Quasipersistent soft X-ray transients

Thermal relaxation **observed for several sources** up to 10^4 days.

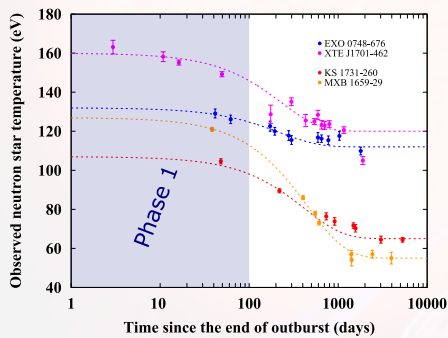


Wijnands et al., J. Astrophys. Astr. 38: 49 (2017)

Studying their cooling curve $T_{\text{eff}}^{\infty}(t)$ allows to probe the crust !

Cooling curve

Mapping between the cooling curve $T_{\text{eff}}^{\infty}(t)$ and the interior of the neutron star.

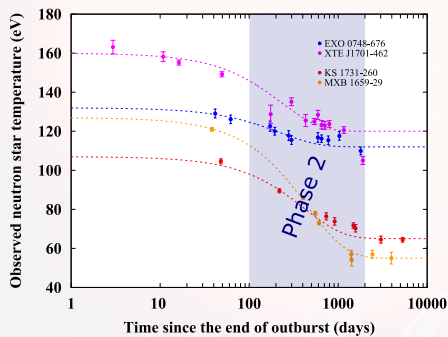


- **Phase 1:** sensitive to the **outer crust**.

Wijnands et al., J. Astrophys. Astr. 38: 49 (2017)

Cooling curve

Mapping between the cooling curve $T_{\text{eff}}^{\infty}(t)$ and the interior of the neutron star.

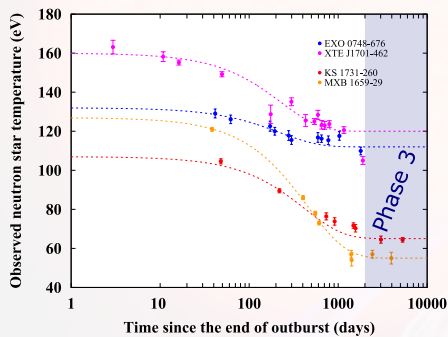


- **Phase 1:** sensitive to the **outer crust**.
- **Phase 2:** sensitive to the **inner crust**.

Wijnands et al., J. Astrophys. Astr. 38: 49 (2017)

Cooling curve

Mapping between the cooling curve $T_{\text{eff}}^{\infty}(t)$ and the interior of the neutron star.



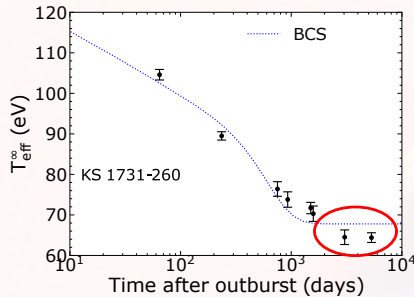
- **Phase 1:** sensitive to the **outer crust**.
- **Phase 2:** sensitive to the **inner crust**.
- **Phase 3:** sensitive to the **outer core** \Rightarrow Thermal equilibrium.

Wijnands et al., J. Astrophys. Astr. 38: 49 (2017)

Observational puzzle: KS 1731–260

KS 1731–260 was found **colder than expected** after ~ 3000 days.

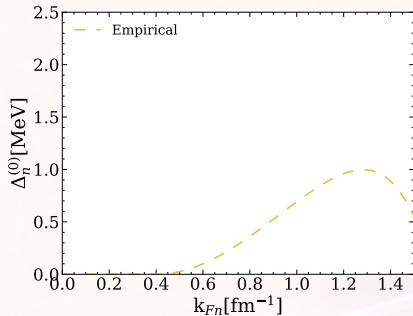
Cackett *et al.*, *ApJL*, 722: L137 (2010)



Observational puzzle: KS 1731–260

KS 1731–260 was found **colder than expected** after ~ 3000 days.

Cackett *et al.*, *ApJL*, 722: L137 (2010)



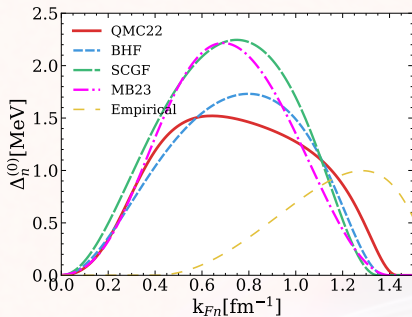
An **Empirical** neutron pairing gap $\Delta_n^{(0)}$ can be inferred from its cooling.

Turlione *et al.*, *A&A*, 577: A5 (2015)

Observational puzzle: KS 1731–260

KS 1731–260 was found **colder than expected** after ~ 3000 days.

Cackett *et al.*, *ApJL*, 722: L137 (2010)



An **Empirical** neutron pairing gap $\Delta_n^{(0)}$ can be inferred from its cooling.

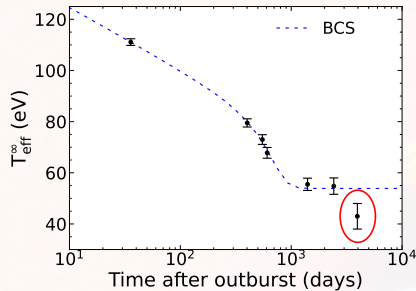
Turlione *et al.*, *A&A*, 577: A5 (2015)

BUT this empirical gap is **not compatible with latest microscopic calculations** based on different many-body approaches !

Observational puzzle: MXB 1659–29

MXB 1659–29 showed an **unexpected** late-time temperature drop.

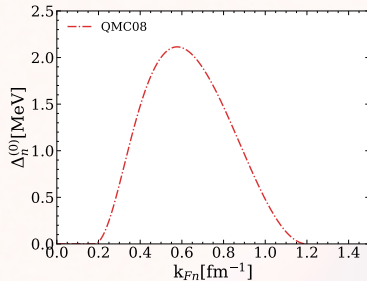
Cackett *et al.*, *ApJ*, 774: 131 (2013)



Observational puzzle: MXB 1659–29

MXB 1659–29 showed an **unexpected** late-time temperature drop.

Cackett *et al.*, *ApJ*, 774: 131 (2013)



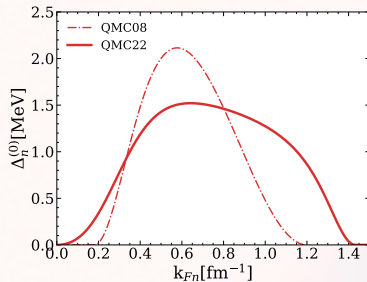
Data can be fitted considering a vanishing $\Delta_n^{(0)}$ at high densities.

Deibel *et al.*, *ApJ*, 839: 95 (2017); Gandolfi *et al.*, *PRL* 101: 132501 (2008)

Observational puzzle: MXB 1659–29

MXB 1659–29 showed an **unexpected** late-time temperature drop.

Cackett *et al.*, *ApJ*, 774: 131 (2013)



Data can be fitted considering a vanishing $\Delta_n^{(0)}$ at high densities.

Deibel *et al.*, *ApJ*, 839: 95 (2017); Gandolfi *et al.*, *PRL* 101: 132501 (2008)

BUT this $\Delta_n^{(0)}$ is **contradicted by recent results from the same group !**

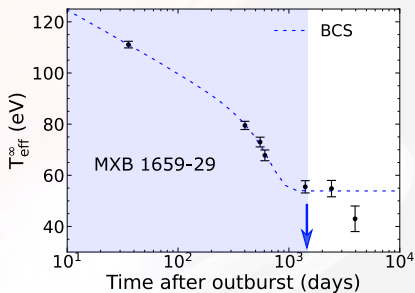
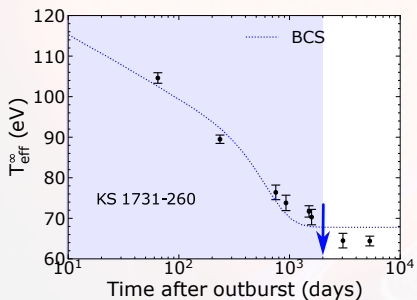
Gandolfi *et al.*, *Condensed Matter*, 7 (2022)

Specific heat and thermal timescale

Thermal timescale

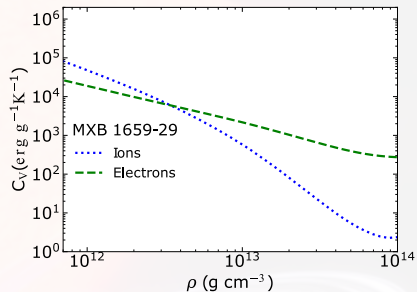
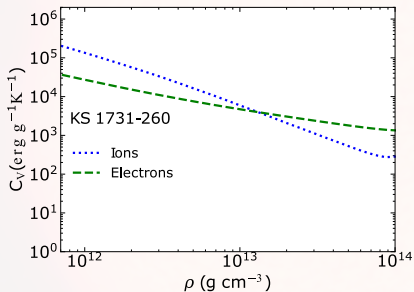
During quiescence, the heat diffuses over a timescale: $\tau_{\text{th}} \propto C_V/\kappa_e$ (κ_e = electronic thermal conductivity and C_V = crustal specific heat).

Page and Reddy, PRL 111, 241102 (2013)



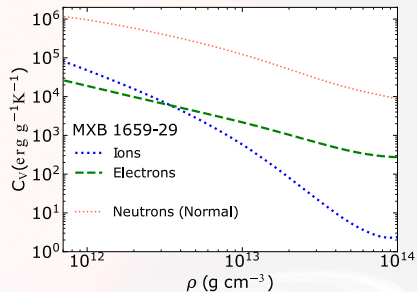
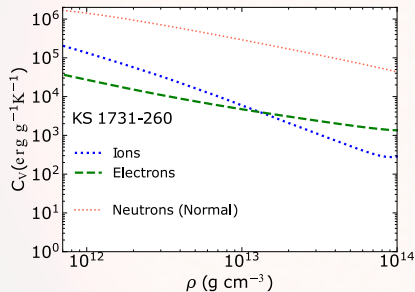
The thermal timescale is too low \Rightarrow Need to increase τ_{th} .

Specific heat and thermal timescale



Within standard cooling models, the neutron contribution to the specific heat is exponentially suppressed !

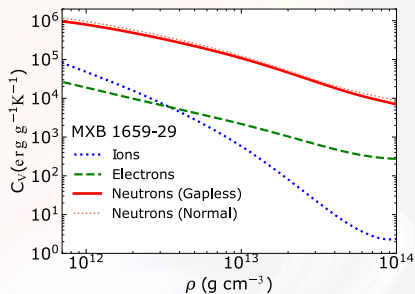
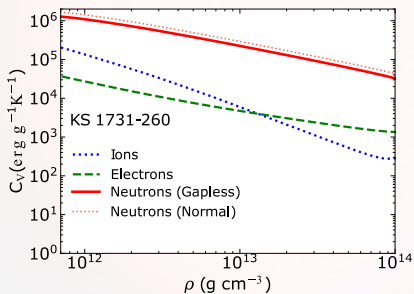
Specific heat and thermal timescale



Neutrons in normal phase give the major contribution to the crustal specific heat !

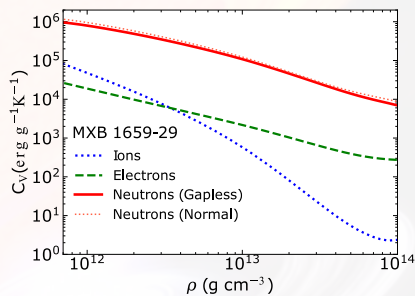
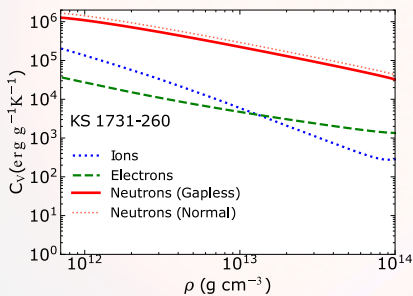
Specific heat and thermal timescale

Gapless superfluidity also gives the major contribution to the crustal specific heat \Rightarrow Impact on the cooling !



Specific heat and thermal timescale

Gapless superfluidity also gives the major contribution to the crustal specific heat \Rightarrow Impact on the cooling !

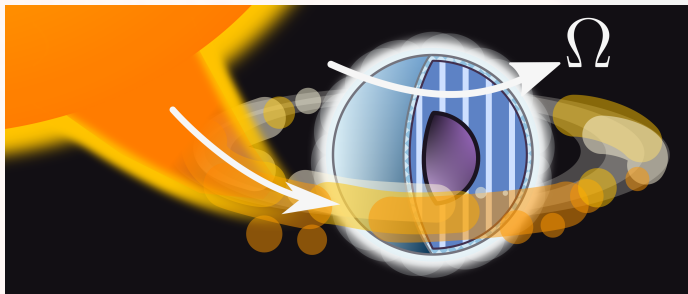


Question

How do we obtain finite V_n ?

Origin of the relative flow in neutron stars

Previous cooling studies ignored currents BUT...



Recycling scenario

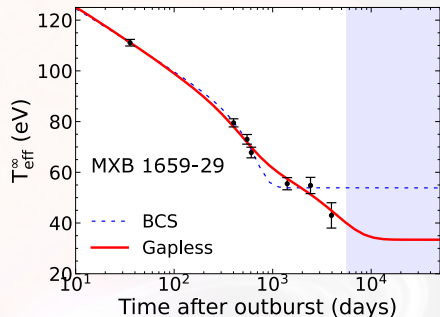
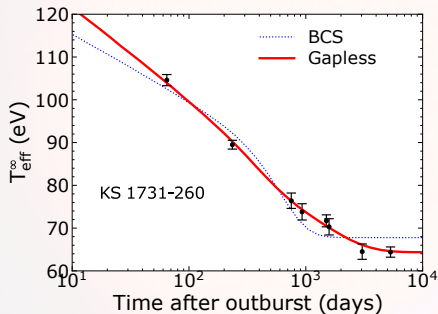
Accretion spins up the neutron star crust \Rightarrow Increase of V_n .

M. A., Alpar et al., Nature, 300:728 (1982)

..

Observational evidence of gapless superfluidity

Within standard cooling models, the thermal relaxation of the crust is too fast.

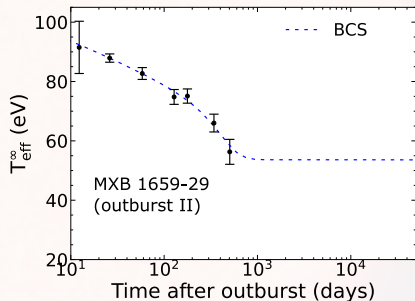


Gapless superfluidity can naturally explain the observed late-time cooling due to the delayed thermal relaxation of the crust.

Allard and Chamel, PRL 132, 181001 (2024)

Consistency check: second outburst of MXB 1659–29

In 2015, MXB 1659–29 entered its **second outburst**.

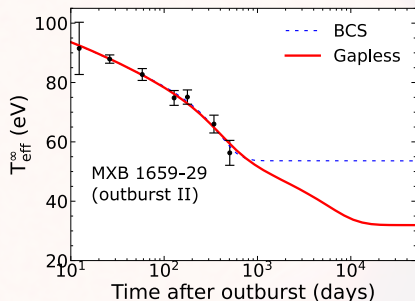


The subsequent cooling phase has been studied within the traditional cooling model.

Parikh *et al.*, *A&A* 624, A84 (2019)

Consistency check: second outburst of MXB 1659–29

In 2015, MXB 1659–29 entered its **second outburst**.



The subsequent cooling phase has been studied within the traditional cooling model.

Parikh *et al.*, A&A 624, A84 (2019)

Gapless superfluidity is also consistent with this cooling phase BUT different prediction at late time.

Conclusions

Microscopic inputs

- Self-Consistent calculations of Δ_q and $\rho_{qq'}$ (entrainment).
Allard and Chamel, PRC 103, 025804 (2021)
- Universal relations and approximate expressions.
Allard and Chamel, Universe 2021, 7(12), 470

Conclusions

Microscopic inputs

- Self-Consistent calculations of Δ_q and $\rho_{qq'}$ (entrainment).
Allard and Chamel, PRC 103, 025804 (2021)
- Universal relations and approximate expressions.
Allard and Chamel, Universe 2021, 7(12), 470

Neutron star cooling

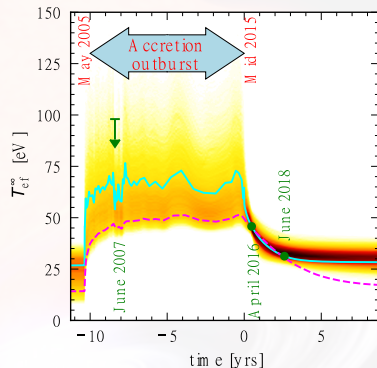
- Order parameter ($\propto \Delta_q$) \neq Quasiparticle energy gap \implies Impact on the specific heat and appearance of a normal fluid (at $T = 0$).
Allard and Chamel, PRC 108, 015801 (2023); Allard and Chamel, PRC 108, 045801 (2023)
- Gapless superfluidity is compatible with the late-time cooling of KS 1731–260 and MXB 1659–29.
Allard and Chamel, PRL 132, 181001 (2024)

Prospects

Another system exhibits peculiar features

HETE J 1900.1–2455

- **High specific heat required:** "[...] *a significant fraction of the dense core is not superfluid/superconductor.*"
Degenaar et al., MNRAS 508 (2021)
- But **only 2 observations...**



To clarify

Further observations are expected!

Prospects

Neutron vortices

Astrophysical manifestations of gapless superfluidity call for further studies of vortex dynamics in neutron star crusts and cores.

Inclusion of rotation: 1D equations \Rightarrow 2D equations

- Beznogov et al., *Astrophys. J.*, 942:72 (2023): NSCool updated to solve fully general relativistic 2D axisymmetric cooling equations (Complex time-dependent evolution of the temperature).
- Ascenzi et al., arXiv:2401.15711 (2024): 3D code designed to study the magneto-thermal evolution of isolated neutron stars.

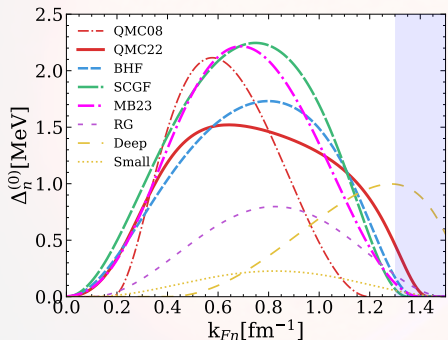
These works are focused on isolated neutron stars: a self-consistent treatment of neutron star cooling and rotation in the context of accreting systems remains to be performed.

Thank you !

Backup slides

1S_0 neutron pairing

Neutron pairing gap computed using various N-body methods:



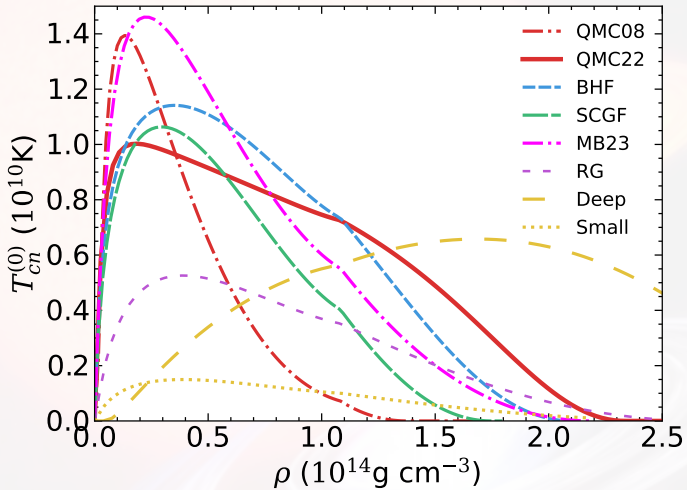
(Dashed box = Fermi wavevectors prevailing in neutron star core)

- **QMC08:** S. Gandolfi et al, Phys. Rev. Lett. **101** (2008).
- **QMC22:** S. Gandolfi et al, Condens. Matter, **7(1)** (2022).
- **BHF:** L. G. Cao et al, Phys. Rev. C **74** (2006).
- **SCGF:** M. Drissi and A. Rios, Eur. Phys. J. A **58** (2022).
- **MB23:** E. Krotscheck et al, arXiv.2305.07096 (2023)
- **Deep and Small:** A. Turlione et al, A&A **577** (2015).

1S_0 neutron pairing

- **RG (Schwenk, Brown et al. 2003):** (One-loop) Renormalization Group equations for PNM. Medium polarization taken into account and self-energy contributions included (in a simple approximation).
- **QMC08 (Gandolfi et al. 2008):** Monte-Carlo computation by solving the many-body problem with a realistic interaction (containing Argonne v_8' (AV8') the two-nucleon interaction and the Urbana IX (UIX) three-nucleon interaction). Medium polarization effects included.
- **QMC22 (Gandolfi et al. 2022):** Most recent Monte-Carlo computation by solving the many-body problem using AV8'+UIX interaction BUT using a better starting trial wavefunction (taking more essential superfluid ground-state correlations into account than it does for QMC08).
- **BHF (Cao et al. 2006):** Brueckner Hartree-Fock computation, considering medium polarization and self-energy effects.
- **SCGF (Drissi et al. 2022):** Pairing gap computed beyond BCS+HF approximation + Three body-forces and medium effects (such as screening terms) and short-range correlations.
- **MB23 (Krotscheck et al.):** Inclusion of many-body effects through diagrammatic methods.

Critical temperatures



Cooling curve

1-to-1 mapping between the cooling curve $T_{\text{eff}}^{\infty}(t)$ and the NS interior.

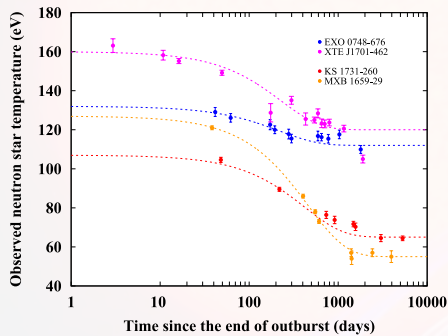
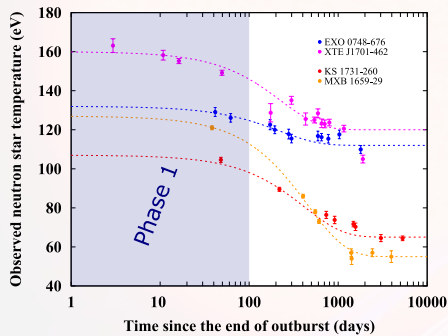


(Figure from R. Wijnands et al, J. Astrophys.
Astr. 38 (2017))

Cooling curve

1-to-1 mapping between the cooling curve $T_{\text{eff}}^{\infty}(t)$ and the NS interior.

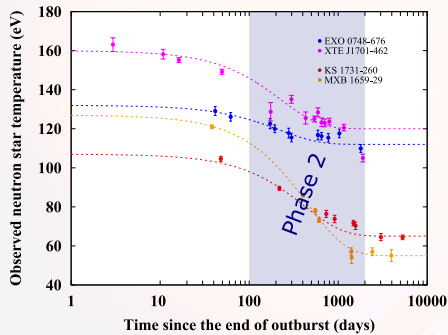


- **Phase 1:** T_{eff}^{∞} sensitive to the outer crust.

(Figure from R. Wijnands et al, J. Astrophys.
Astr. 38 (2017))

Cooling curve

1-to-1 mapping between the cooling curve $T_{\text{eff}}^{\infty}(t)$ and the NS interior.



- **Phase 1:** T_{eff}^{∞} sensitive to the outer crust.
- **Phase 2:** T_{eff}^{∞} sensitive to the inner crust.

(Figure from R. Wijnands et al, J. Astrophys.
Astr. 38 (2017))

Cooling curve

1-to-1 mapping between the cooling curve $T_{\text{eff}}^{\infty}(t)$ and the NS interior.

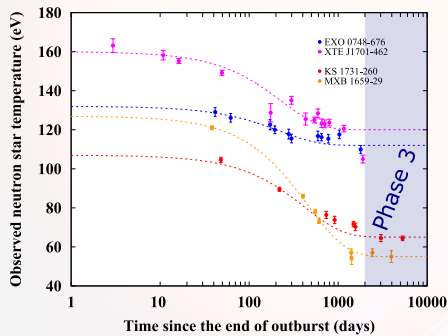


(Figure from R. Wijnands et al, J. Astrophys. Astr. 38 (2017))

- **Phase 1:** T_{eff}^{∞} sensitive to the outer crust.
- **Phase 2:** T_{eff}^{∞} sensitive to the inner crust.
- **Phase 3:** T_{eff}^{∞} sensitive to the outer core \Rightarrow Thermal equilibrium.

The cooling curve allows to probe the NS interiors.

Pinning forces

Pinning forces

Finite V_n can be sustained by the pinning of quantized vortices BUT pinning forces f_{pin} compete against Magnus forces $f_{\text{Magnus}} \implies$ Existence of V_{cr} .

- f_{pin} differs by orders of magnitude.
- Averaging procedure over many vortices and pinning sites (model dependent).
- Vortices can pin to proton fluxons in the core (additional pinning sites: $f_{\text{pin}} \nearrow$).
- Landau's velocity can be suppressed significantly by the presence of clusters (Miller et al., Phys. Rev. Lett. 99, 070402 (2007)).

Astrophysical manifestations of gapless superfluidity call for further studies of vortex dynamics in neutron star crusts and cores.

Estimates of V_{cr}

The lag $\mathbb{V}_n \simeq V_n$ is limited by the critical lag V_{cr} beyond which vortices are unpinned.

- Melatos & Millhouse, ApJ, 948(2), 106 (2023) (Statistical analysis of 541 glitches and 177 pulsars): $V_{\text{cr}} \sim 10^5 \text{ cm s}^{-1}$ BUT no pinning in the core.
- Pizzochero, ApJL 743(1), 20 (2011) (straight parallel vortices pinned to the crust):

$$V_{\text{cr}} \approx 10^7 (f_p / 10^{18} \text{ dyn cm}^{-1}) \text{ cm s}^{-1},$$

where f_p is the maximum mesoscopically averaged pinning force per unit length.

The theoretical challenges to estimate this force are numerous (see, e.g., Antonopoulou et al., Rep. Prog. Phys. 85(12), 126901 (2022), for a recent review).

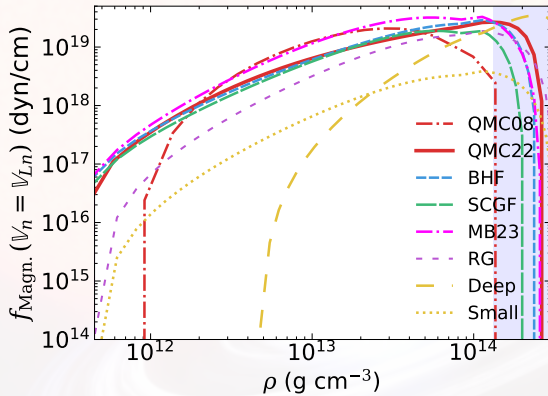
Computing f_p

- Pecak et al., Phys. Rev. C 104, 055801 (2021): internal quantum structure of a vortex locally modified in presence of nuclear clusters \Rightarrow a vortex should be described within a fully self-consistent quantum mechanical approach.
- Klausner et al., Phys. Rev. C 108, 035808 (2023): pinning force (for one single cluster) traditionally determined from static calculations of energy differences.
- Wlazlowski et al., Phys. Rev. Lett. 117(23), 232701 (2016): A more reliable approach consists in calculating the force dynamically BUT no such calculations have been systematically carried out so far !
- Calculations on a mesoscopic scale are more uncertain: results depend on the vortex tension and crustal structure (see, Seveso et al., MNRAS 455(4), 3952–3967 (2016) and Link and Levin, Astrophys. J. 941(2), 148 (2022)). **Estimates of f_p differ by orders of magnitude.**
- Vortices are also expected to pin to proton fluxoids in the deepest layers of the crust or, even, in the core ! (pinning to fluxoids is supported by observations of Crab and Vela pulsar glitches, Sourie and Chamel, MNRAS 493(1), 98–102 (2020)).

Pinning force estimation

The pinning force can be roughly estimated from the Magnus force.

$$f_p(\rho) \approx 2.5 \times 10^{19} \text{ dyn cm}^{-1} \left(\frac{\Delta_n^{(0)}}{1 \text{ MeV}} \right) \left(\frac{\rho Y_{\text{nf}}}{10^{14} \text{ g cm}^{-3}} \right)^{2/3}.$$



Inhomogeneities in the crust and V_{cr}

We can adopt the estimate $f_p \simeq 10^{18} \text{ dyn cm}^{-1}$ (also given in Antonopoulou et al., Rep. Prog. Phys. 85(12), 126901 (2022)) which yields (using the *snowplow model*) $V_{\text{cr}} \sim 10^7 \text{ cm s}^{-1}$.

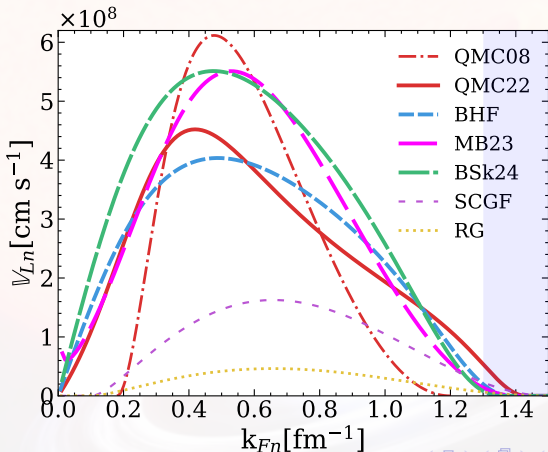
- Landau's velocity $\mathbb{V}_{L_n} \sim 10^8 \text{ cm s}^{-1}$ is one order of magnitude higher than V_{cr} .
- However, the estimates of V_{cr} , \mathbb{V}_{L_n} , and f_p were obtained ignoring the inhomogeneities in the crust.
- Antonelli et al., MNRAS 464(1), 721–733 (2017): crust inhomogeneities increase V_{cr} by a factor $(1 - \varepsilon_n) = m_n^*/m_n$ (with being ε_n = entrainment parameter and m_n^*/m_n = dynamical effective mass).
- Chamel, Phys. Rev. C 85(3), 035801 (2012): $m_n^*/m_n \approx 1 - 14$ (depending on the crustal layer) \implies the maximum V_{cr} could be increased by an order of magnitude !

Having $\mathbb{V}_{L_n} \lesssim V_{\text{cr}}$ is not implausible !

Landau's velocity in neutron matter

Landau's velocity is approximately given by

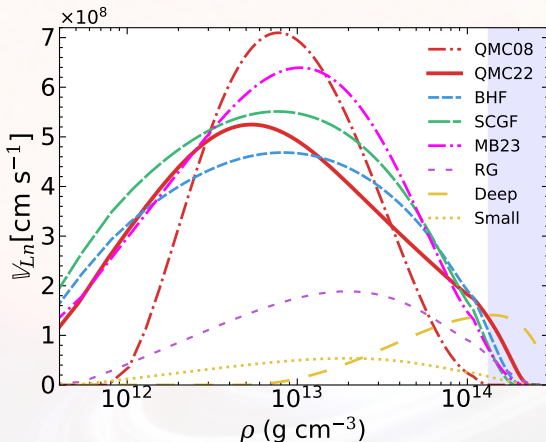
$$V_{Ln} \approx 1.2 \times 10^8 \text{ cm s}^{-1} \left(\frac{\Delta_n^{(0)}}{1 \text{ MeV}} \right) \left(\frac{10^{14} \text{ g cm}^{-3}}{\rho Y_{\text{nf}}} \right)^{1/3}.$$



Landau's velocity in neutron matter

Landau's velocity is approximately given by

$$V_{Ln} \approx 1.2 \times 10^8 \text{ cm s}^{-1} \left(\frac{\Delta_n^{(0)}}{1 \text{ MeV}} \right) \left(\frac{10^{14} \text{ g cm}^{-3}}{\rho Y_{\text{nf}}} \right)^{1/3}.$$

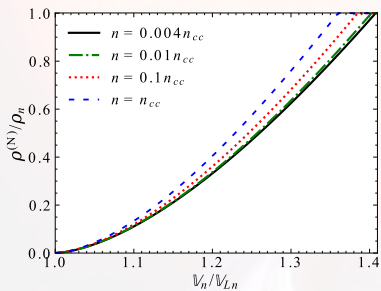


Magnus force in gapless superfluidity

The Magnus force depends on the superfluid density (see, for e.g.; Antonelli et al., In Astrophysics in the XXI Century with Compact Stars, Chap. 7, p219-281 (2022))

$$f_{\text{pin}} \simeq \kappa_n (\rho_n - \rho_n^{(N)}) \mathbb{V}_n .$$

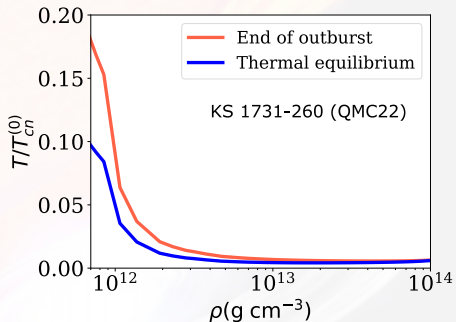
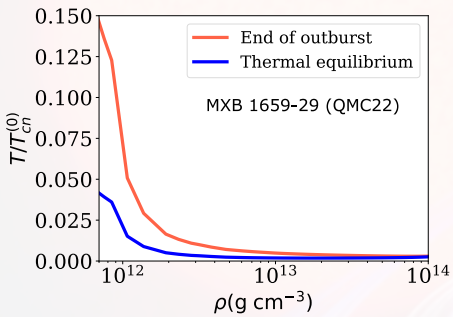
The normal neutron density $\rho_n^{(N)}$ is defined in terms of the entrainment matrix (Allard and Chamel, Phys. Rev. C. 108, 045801 (2023)).



- $\rho_n^{(N)} \rightarrow \rho_n$ with increasing \mathbb{V}_n .
- **Reduction of the pinning force** for increasing \mathbb{V}_n in gapless superfluidity.

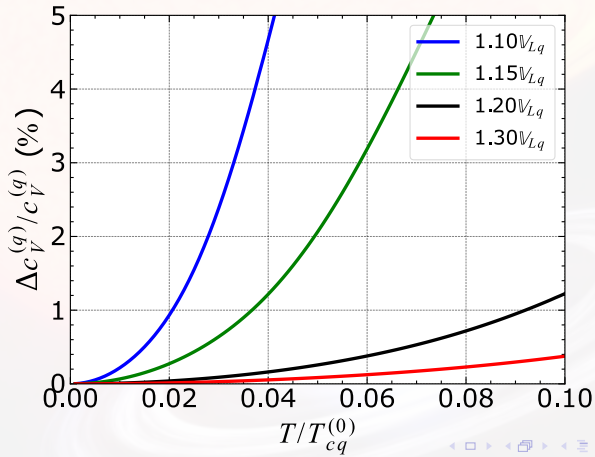
Low-temperature approximation ?

Highest temperatures reached at $\sim 0.15 - 0.20 T_{cn}^{(0)}$, at the end of outburst in the shallowest regions of the crust.



Low-temperature approximation ?

(Relative) errors not exceeding 2.9% (for MXB) and 0.028% (for KS) in shallowest regions. For the deeper layers, errors do not exceed 0.01% !



Energy-density functional theory with currents

The dynamic of neutron-proton mixtures is governed by the **time-dependent Hartree-Fock Bogoliubov (TDHFB) equations**

$$i\hbar\partial_t n_q(\mathbf{r}\sigma, \mathbf{r}'\sigma', t) = h_q(\mathbf{r}, t)n_q(\mathbf{r}\sigma, \mathbf{r}'\sigma', t) - h_q^*(\mathbf{r}', t)\tilde{n}_q(\mathbf{r}\sigma, \mathbf{r}'\sigma', t) \\ + \sigma\sigma'\tilde{\Delta}_q(\mathbf{r}, t)\tilde{n}_q(\mathbf{r} - \sigma, \mathbf{r}' - \sigma', t) - \tilde{n}_q(\mathbf{r}\sigma, \mathbf{r}'\sigma', t)\tilde{\Delta}_q^*(\mathbf{r}', t)$$

with single-particle hamiltonian (depending on densities, **effective mass** and **currents**)

$$h_q(\mathbf{r}, t) = -\nabla \cdot \frac{\hbar^2}{2m_q^\oplus(\mathbf{r}, t)}\nabla + U_q(\mathbf{r}, t) + \frac{1}{2i} [\mathbf{I}_q(\mathbf{r}, t) \cdot \nabla + \nabla \cdot \mathbf{I}_q(\mathbf{r}, t)]$$

with potentials defined through particle density $n_q(\mathbf{r}\sigma, \mathbf{r}'\sigma', t)$ and pair density matrices $\tilde{n}_q(\mathbf{r}\sigma, \mathbf{r}'\sigma', t)$,

$$\frac{\hbar^2}{2m_q^\oplus(\mathbf{r}, t)} = \frac{\delta E}{\delta \tau_q(\mathbf{r}, t)}, \quad U_q(\mathbf{r}, t) = \frac{\delta E}{\delta n_q(\mathbf{r}, t)}, \quad \mathbf{I}_q(\mathbf{r}, t) = \frac{\delta E}{\delta \mathbf{j}_q(\mathbf{r}, t)},$$

$$\tilde{\Delta}_q(\mathbf{r}, t) = \Delta_q(\mathbf{r}, t)e^{i\phi_q(\mathbf{r}, t)} = 2\frac{\delta E}{\delta \tilde{n}_q^*(\mathbf{r}, t)}.$$

Mass currents

A **continuity equation** can be derived from the TDHFB equations (Allard and Chamel in Phys. Rev. C. 100, 065801 (2019) and Phys. Rev. C. 103, 025804 (2021))

$$\partial_t (m_q n_q(\mathbf{r}, t)) + \nabla \cdot \boldsymbol{\rho}_q(\mathbf{r}, t) = 0$$

Mass current $\boldsymbol{\rho}_q$

$$\boldsymbol{\rho}_q(\mathbf{r}, t) = m_q n_q(\mathbf{r}, t) \left(\frac{\hbar \mathbf{j}_q(\mathbf{r}, t)}{m_q^\oplus(\mathbf{r}, t) n_q(\mathbf{r}, t)} + \frac{\mathbf{I}_q(\mathbf{r}, t)}{\hbar} \right) = m_q n_q(\mathbf{r}, t) \mathbf{v}_q(\mathbf{r}, t)$$

Which allows to define the **true velocity** as $\mathbf{v}_q(\mathbf{r}, t) = \boldsymbol{\rho}_q(\mathbf{r}, t) / (m_q n_q(\mathbf{r}, t))$

- Does not explicitly depend on the pairing gap $\widetilde{\Delta}_q$.
- **General** case: valid for both uniform and non-uniform systems.

Homogeneous solutions: finite T and finite currents

Focusing on hot **homogeneous neutron-proton superfluid mixture** with stationary flows in normal fluid rest frame ($\mathbf{v}_N = \mathbf{0}$), **TDHFB can be solved exactly** (Allard and Chamel, Phys. Rev. C. 103, 025804 (2021)) !

$$\varepsilon_{\mathbf{k}}^{(q)} = \hbar \mathbf{k} \cdot \mathbb{V}_{\mathbf{q}} + \sqrt{\varepsilon_{\mathbf{k}}^{(q)2} + \Delta_q^2}, \quad \varepsilon_{\mathbf{k}}^{(q)} = \frac{\hbar^2 \mathbf{k}^2}{2m_q^{\oplus}} - \mu_q,$$

Effective superfluid velocity

$$\mathbb{V}_{\mathbf{q}} = \frac{m}{m_q^{\oplus}} \mathbf{V}_{\mathbf{q}} + \frac{\mathbf{I}_{\mathbf{q}}}{\hbar} \neq \mathbf{v}_{\mathbf{q}}$$

- $\mathbb{V}_{\mathbf{q}}$ contains the mutual contributions of \mathbf{V}_n and \mathbf{V}_p .
- **Dynamical decoupling** between quantities associated with protons or neutrons.

Homogeneous solutions: $T = 0$ K and small currents

For homogeneous neutron-proton superfluid mixture, **at low temperatures and small currents**, the normal component disappears ($\mathbf{v}_N = 0$)

$$\rho_n = \rho_{nn}^{(\text{TDHF})} \mathbf{V}_n + \rho_{np}^{(\text{TDHF})} \mathbf{V}_p, \quad \rho_p = \rho_{pp}^{(\text{TDHF})} \mathbf{V}_p + \rho_{pn}^{(\text{TDHF})} \mathbf{V}_n$$

The entrainment matrix becomes **independent of pairing** \Rightarrow TDHF !

(Chamel and Allard, Phys. Rev. C 100, 065801 (2019))

$$\rho_{np}^{(\text{TDHF})} = \rho_{pn}^{(\text{TDHF})} = \frac{1}{4} mn(1 - \eta^2) \left(1 - \frac{\mathbf{m}}{\mathbf{m}_V^\oplus} \right)$$

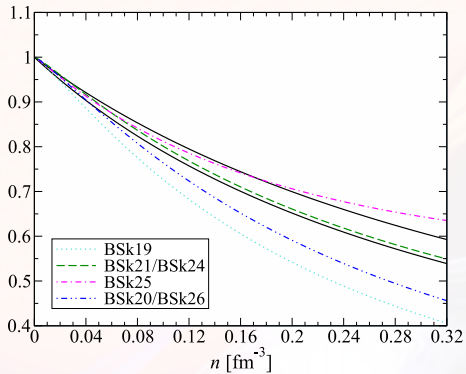
$$\rho_{nn}^{(\text{TDHF})} = \frac{1}{2} mn(1 + \eta) - \rho_{np}^{(\text{TDHF})}, \quad \rho_{pp}^{(\text{TDHF})} = \frac{1}{2} mn(1 - \eta) - \rho_{np}^{(\text{TDHF})}.$$

with $n = (n_n + n_p)$ the total density and $\eta = (n_n - n_p)/n$ the isospin asymmetry.

The entrainment matrix is parametrized by the **isovector effective mass**!

Homogeneous solutions: $T = 0$ K and small currents

Isovector effective mass is also related to **giant resonances in atomic nuclei !**



Its density dependence is still uncertain !

Superfluid hydrodynamics and entrainment effects

Similarly to superfluid $^3\text{He}-^4\text{He}$ mixture (Andreev and Bashkin, Sov. Phys. JETP 42, 164 (1975)), **superfluid neutrons (n) and protons (p) in a neutron star** are mutually coupled by non-dissipative **entrainment effects** (Gusakov and Haensel, Nucl. Phys. A, 761:333–348 (2005)).

Mass current and velocity fields (superfluid mixtures)

Mass currents ρ_q (with $q = n, p$) are not simply aligned to their associated superfluid velocities V_q .

$$\rho_n = \rho_n^{(N)} v_N + \rho_{nn} V_n + \rho_{np} V_p ,$$

$$\rho_p = \rho_p^{(N)} v_N + \rho_{pp} V_p + \rho_{pn} V_n ,$$

$\rho_{qq'}$ = **Entrainment matrix** $\rho_q^{(N)}$ = **Normal density**

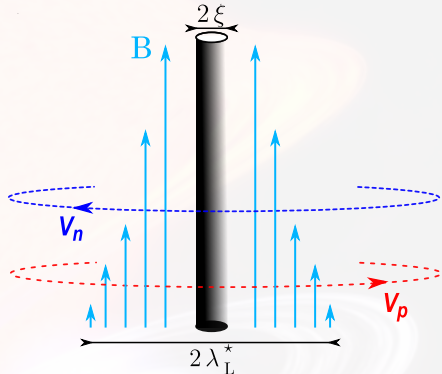
Superfluid hydrodynamics and entrainment effects

Entrainment effects induce a **circulation of protons around neutron vortices**.

Neutron vortices carry a magnetic flux Φ^* :

$$\Phi^* = \frac{hc}{2|e|} \frac{\rho_{np}}{\rho_{pp}}.$$

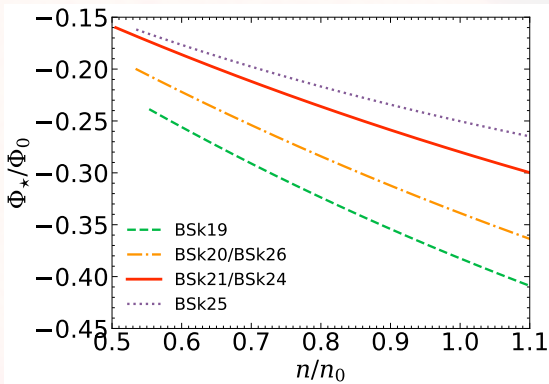
(Sedrakyan and Shakhabasyan, Astrofizika 8, 557 (1972); ibid. 16, 727 (1980))



Electrons scatter off the induced magnetic flux \Rightarrow strong coupling between the core superfluid and the crust (Alpar, Langer, Sauls, ApJ 282, 533 (1984)).

Neutron vortex magnetization

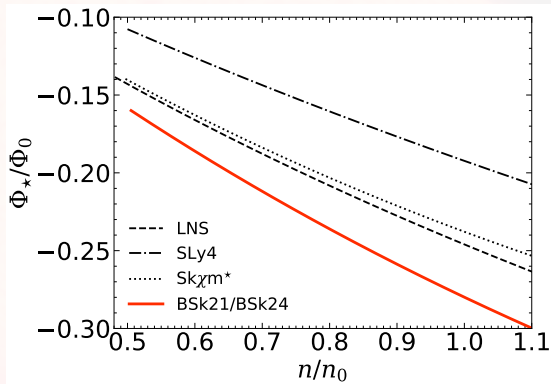
Exact solution for zero temperature and small currents ($\mathbb{V}_q \leq \mathbb{V}_{Lq}$).



For $T \neq 0$ or higher velocities (i.e. $\mathbb{V}_q > \mathbb{V}_{Lq}$), computing the vortex magnetic flux Φ^* involves additional contributions coming from the normal fluid.

Neutron vortex magnetization

Exact solution for zero temperature and small currents ($\mathbb{V}_q \leq \mathbb{V}_{Lq}$).



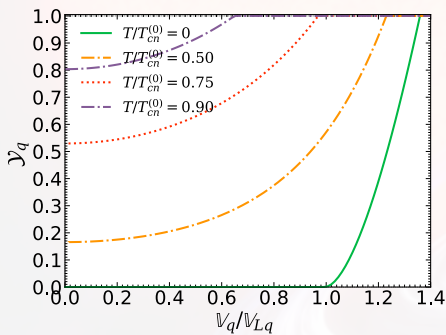
For $T \neq 0$ or higher velocities (i.e. $\mathbb{V}_q > \mathbb{V}_{Lq}$), computing the vortex magnetic flux Φ^* involves additional contributions coming from the normal fluid.

Mass current and generalized Yosida functions

The true velocity (and mass current) takes a simple form

$$\mathbf{v}_q = \left(1 - \mathcal{Y}_q(T, \mathbb{V}_q)\right) \mathbb{V}_q$$

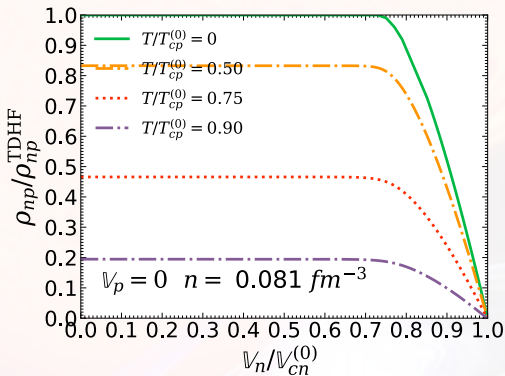
With \mathcal{Y}_q , the **generalized Yosida functions** (universal after using \mathbb{V}_q and rescaling)



Interpolating functions available
(Allard and Chamel, Universe 7(12) (2021)) !

Entrainment matrix: finite T and finite currents

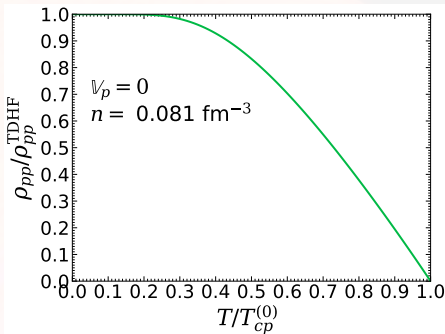
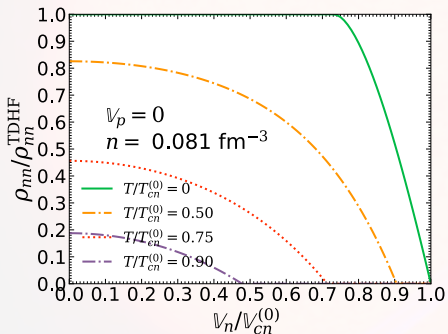
Entrainment matrix numerically computed in Allard and Chamel, Universe 7(12) (2021) (Protons coupled with the rest of the star: $v_p = \nabla_p = 0$).



Generalization of the **superfluid mass densities** for mixtures !

Entrainment matrix: finite T and finite currents

Entrainment matrix numerically computed in Allard and Chamel, Universe 7(12) (2021) (Protons coupled with the rest of the star: $v_p = \nabla_p = 0$).

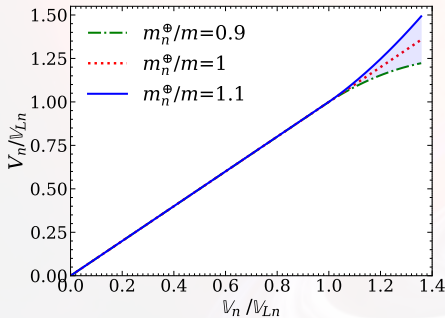


Generalization of the **superfluid mass densities** for mixtures !

Velocities

Three kind of velocities

- Superfluid velocity V_q : Rescaled **momentum**.
- Effective superfluid velocity \mathbb{V}_q : **Dynamical decoupling** between neutrons and protons.
- True velocity v_q : Velocity of **mass-transport** of nucleons.

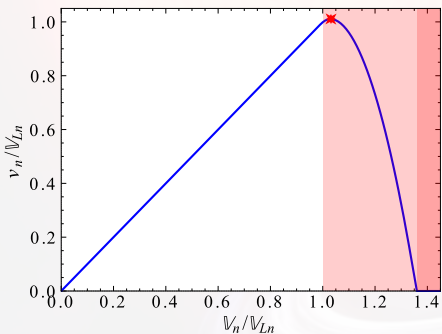


Example: Results obtained from neutron matter ($n_p = 0$) \Rightarrow
Non-linear universal relations
(beyond Landau's velocity)!

Velocities

Three kind of velocities

- Superfluid velocity V_q : Rescaled **momentum**.
- Effective superfluid velocity \mathbb{V}_q : **Dynamical decoupling** between neutrons and protons.
- True velocity v_q : Velocity of **mass-transport** of nucleons.



Example: neutron matter

Non-linear universal relations
(beyond Landau's velocity)!

Crustcool code

Study of the thermal evolution using crustcool (A. Cummings).

- Same microphysics as Brown et al., *Astrophys. J.*, 698: 1020–1032 (2009) BUT
- Modified neutron specific heat & parameterized with V_n + Approximate formula for the critical velocities.
- Implementation of neutron diffusion.

Crustcool code

Study of the thermal evolution using crustcool (A. Cummings).

- Same microphysics as Brown et al., *Astrophys. J.*, 698: 1020–1032 (2009) BUT
- Modified neutron specific heat & parameterized with \mathbb{V}_n + Approximate formula for the critical velocities.
- Implementation of neutron diffusion.

Parameters

- Accretion duration $t_{\text{accretion}}$ and accretion rate \dot{m} .
- Neutron star mass M_{NS} and radius R_{NS} .
- Core temperature (at thermal equilibrium) T_{core} and temperature at the basis of the envelope T_{base} .
- Impurity parameter Q_{imp} entering the thermal conductivity.
- (Effective) superfluid velocity \mathbb{V}_n entering the neutron specific heat.

Crustcool code

Study of the thermal evolution using crustcool (A. Cummings).

- Same microphysics as Brown et al., *Astrophys. J.*, 698: 1020–1032 (2009) BUT
- Modified neutron specific heat & parameterized with \mathbb{V}_n + Approximate formula for the critical velocities.
- Implementation of neutron diffusion.

Parameters

- Accretion duration $t_{\text{accretion}}$ and accretion rate \dot{m} .
- Neutron star mass M_{NS} and radius R_{NS} .
- Core temperature (at thermal equilibrium) T_{core} and temperature at the basis of the envelope T_{base} .
- Impurity parameter Q_{imp} entering the thermal conductivity.
- (Effective) superfluid velocity \mathbb{V}_n entering the neutron specific heat.

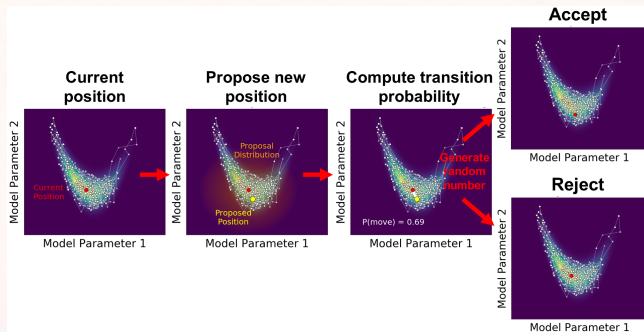
Fixed $t_{\text{accretion}}$, \dot{m} , M_{NS} and R_{NS} and $(\mathbb{V}_n, T_{\text{core}}, T_{\text{base}}, Q_{\text{imp}})$ being free parameters.

crustcool code

- **Composition:** Haensel & Zdunik, A&A 229 (1990).
- **Thermal conductivity:** Fortran subroutine `condegin` (Potekhin, <http://www.ioffe.ru/astro/conduct/condin.html>).
- **Pressure :** Degenerate et relativistic electrons (Paczynski ApJ 267 (1983)) + Non-relativistic degenerate neutrons (Mackie & Baym, Nucl. Phys. A 285 (1977)) + Ionic and radiative pressures neglected.
- **Specific heat:** Electrons in normal phase + Gapless neutrons (Fermi energy from Mackie & Baym, Nucl. Phys. A 285 (1977)) + Ionic contribution (solid ions, G. Chabrier, ApJ 414 (1993)).

Markov-Chain Monte-Carlo (MCMC)

The parameter space is probed through **Markov-Chain Monte-Carlo** (MCMC) method.



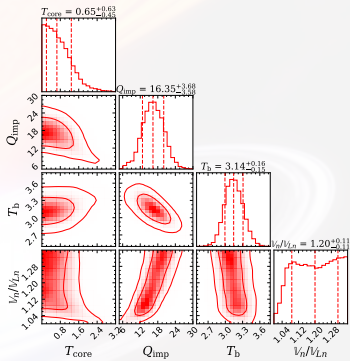
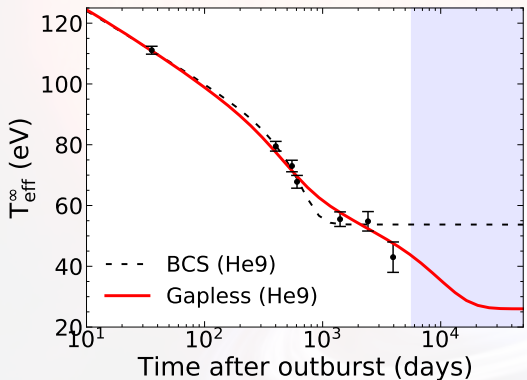
Complex probability distributions are approximated through random steps to generate samples of the desired probability distribution.

Last observation point of MXB 1659–29 (outburst I)

Results obtained for Haensel & Zdunik (1990) with neutron diffusion.

Cooling of MXB 1659–29 (outburst I)

Four possible values for the last data point: $k_B T_{\text{eff}}^\infty = 43 \pm 5$ eV.

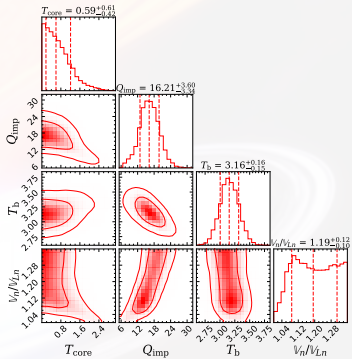
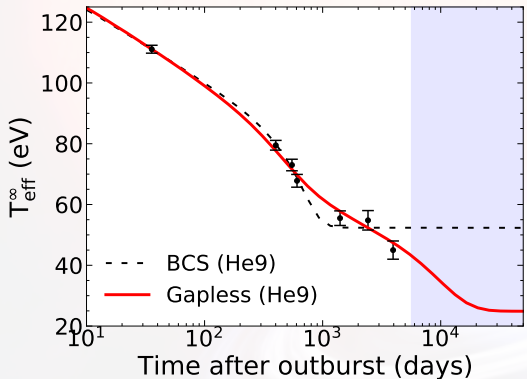


Last observation point of MXB 1659–29 (outburst I)

Results obtained for Haensel & Zdunik (1990) with neutron diffusion.

Cooling of MXB 1659–29 (outburst I)

Four possible values for the last data point: $k_B T_{\text{eff}}^{\infty} = 45 \pm 3$ eV.

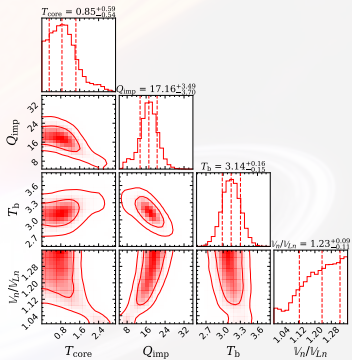
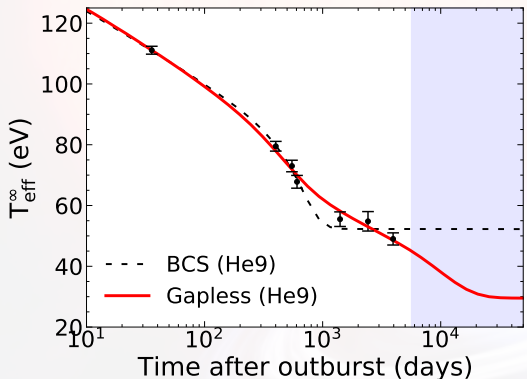


Last observation point of MXB 1659–29 (outburst I)

Results obtained for Haensel & Zdunik (1990) with neutron diffusion.

Cooling of MXB 1659–29 (outburst I)

Four possible values for the last data point: $k_B T_{\text{eff}}^{\infty} = 49 \pm 2$ eV.

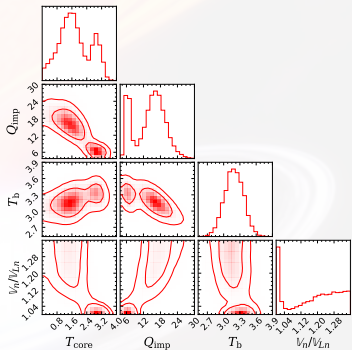
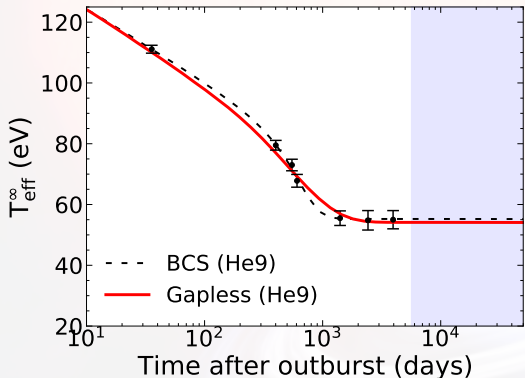


Last observation point of MXB 1659–29 (outburst I)

Results obtained for Haensel & Zdunik (1990) with neutron diffusion.

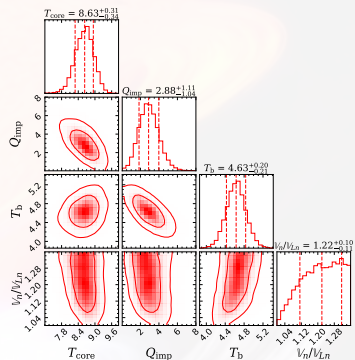
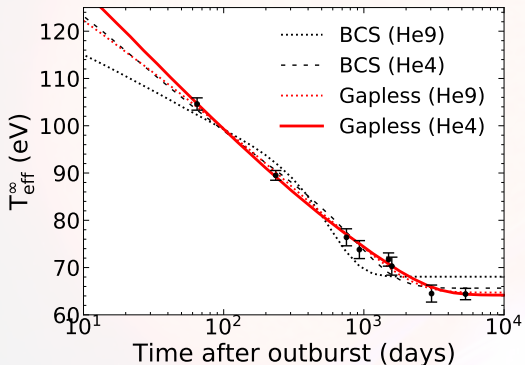
Cooling of MXB 1659–29 (outburst I)

Four possible values for the last data point: $k_B T_{\text{eff}}^{\infty} = 55 \pm 3$ eV.



Cooling with accreted-crust EoS BSk21 (no nHD)

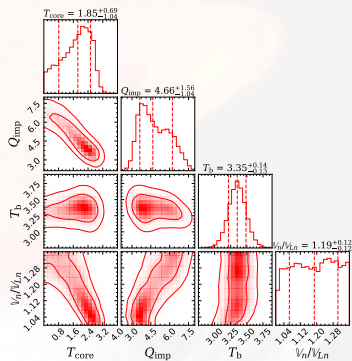
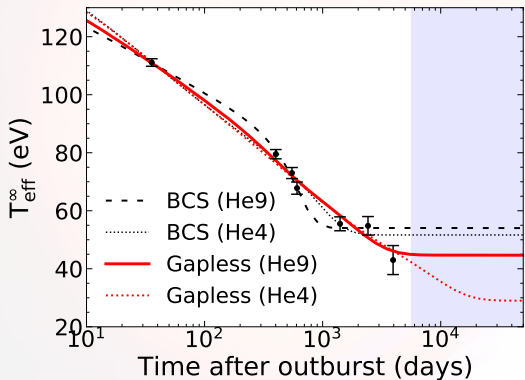
Cooling has been studied with the accreted-crust EoS from Fantina et al. A&A 620, A105 (2018) based on (BSk21).



Gapless superfluidity gives an excellent fit to the cooling data.

Cooling with accreted-crust EoS BSk21 (no nHD)

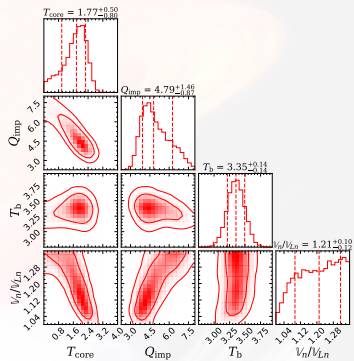
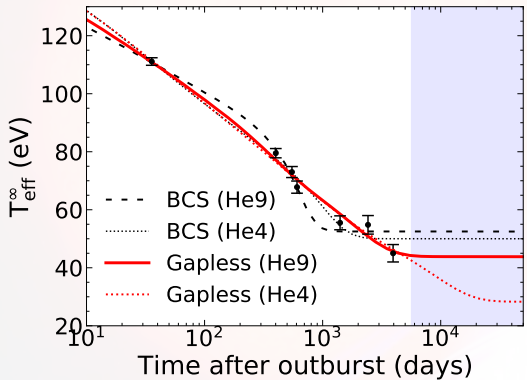
Cooling has been studied with the accreted-crust EoS from Fantina et al. A&A 620, A105 (2018) based on (BSk21).



Gapless superfluidity gives a good fit to the cooling data, for the last point at 43 ± 5 eV.

Cooling with accreted-crust EoS BSk21 (no nHD)

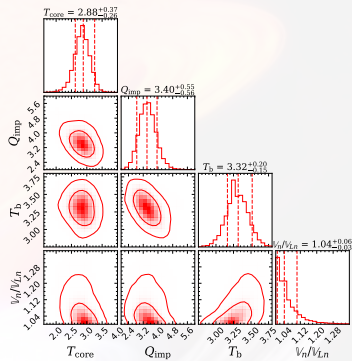
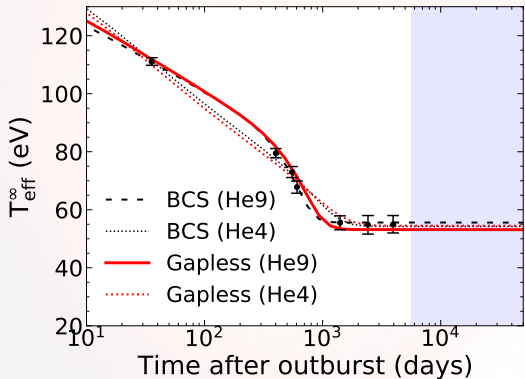
Cooling has been studied with the accreted-crust EoS from Fantina et al. A&A 620, A105 (2018) based on (BSk21).



Gapless superfluidity gives an good fit to the cooling data, for the last point at 45 ± 3 eV.

Cooling with accreted-crust EoS BSk21 (no nHD)

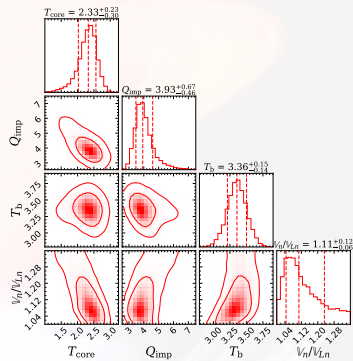
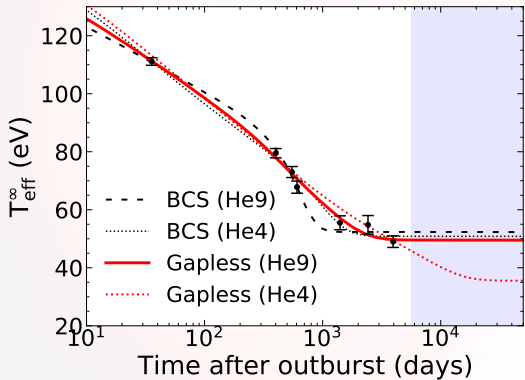
Cooling has been studied with the accreted-crust EoS from Fantina et al. A&A 620, A105 (2018) based on (BSk21).



Gapless superfluidity gives a good fit to the cooling data, for the last point at 55 ± 3 eV.

Cooling with accreted-crust EoS BSk21 (no nHD)

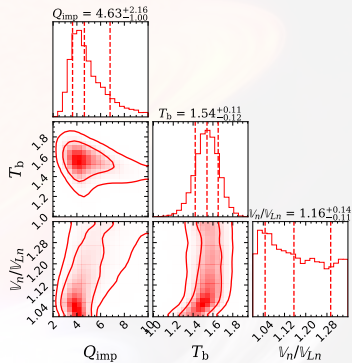
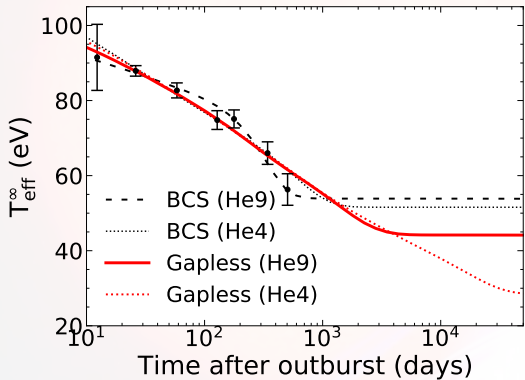
Cooling has been studied with the accreted-crust EoS from Fantina et al. A&A 620, A105 (2018) based on (BSk21).



Gapless superfluidity gives a good fit to the cooling data, for the last point at 49 ± 2 eV.

Cooling with accreted-crust EoS BSk21 (no nHD)

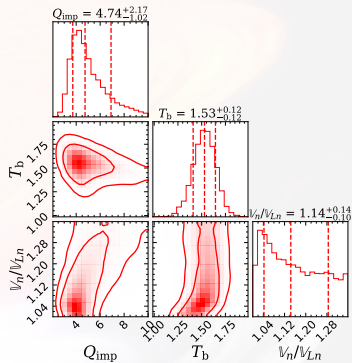
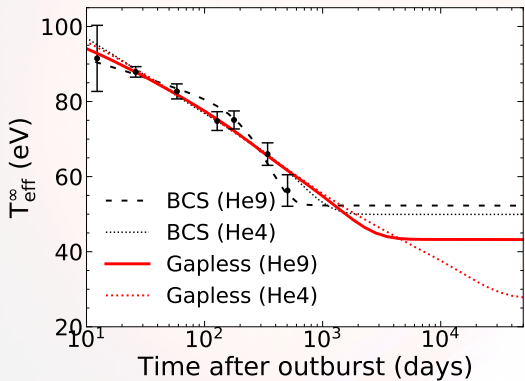
Cooling has been studied with the accreted-crust EoS from Fantina et al. A&A 620, A105 (2018) based on (BSk21).



Gapless superfluidity slightly misses the last data point.

Cooling with accreted-crust EoS BSk21 (no nHD)

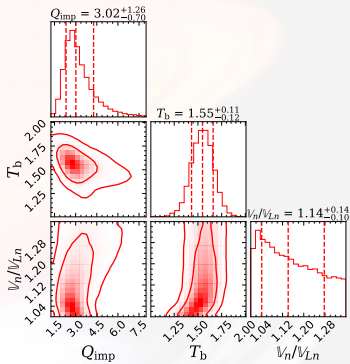
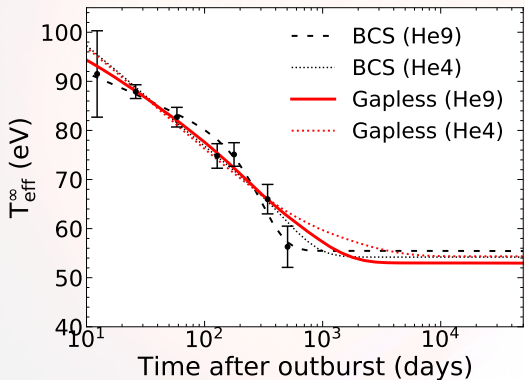
Cooling has been studied with the accreted-crust EoS from Fantina et al. A&A 620, A105 (2018) based on (BSk21).



Gapless superfluidity slightly misses the last data point.

Cooling with accreted-crust EoS BSk21 (no nHD)

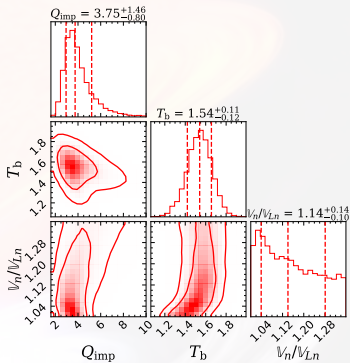
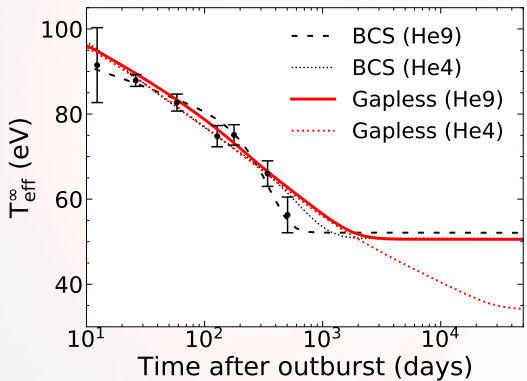
Cooling has been studied with the accreted-crust EoS from Fantina et al. A&A 620, A105 (2018) based on (BSk21).



Gapless superfluidity slightly misses the last data point.

Cooling with accreted-crust EoS BSk21 (no nHD)

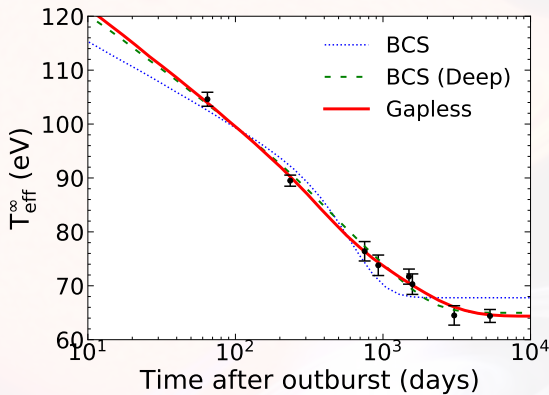
Cooling has been studied with the accreted-crust EoS from Fantina et al. A&A 620, A105 (2018) based on (BSk21).



Gapless superfluidity slightly misses the last data point.

Influence of the Deep gap

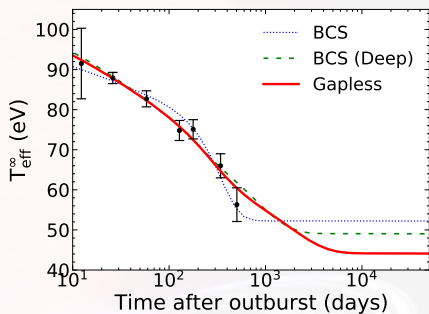
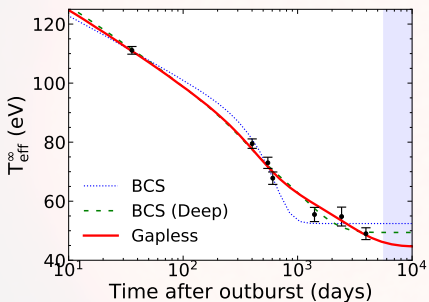
Study of the deep gap (using Haensel & Zdunik (1990), without nHD with He9 envelope model) and $M_{\text{NS}} = 1.62M_{\odot}$ and $R_{\text{NS}} = 11.2 \text{ km}$.



Deep gap (with BCS superfluidity) gives good fit to the cooling data.

Influence of the Deep gap

Study of the deep gap (using Haensel & Zdunik (1990), without nHD with He9 envelope model) and $M_{\text{NS}} = 1.62M_{\odot}$ and $R_{\text{NS}} = 11.2 \text{ km}$.



Deep gap (with BCS superfluidity) gives good fit to the cooling data.